Uplink Interference Management for HetNets Stressed by Uniformly Distributed Wide-Band Jammers

By

Muhammad Qasim

00000280973

Supervisor

Dr. Muhammad Imran

Department of Electrical Engineering

Military College of Signals (MCS)

National University of Sciences and Technology (NUST)

Islamabad, Pakistan

August 2020

Uplink Interference Management for HetNets Stressed by Uniformly Distributed Wide-Band Jammer

By

Muhammad Qasim

00000280973

Supervisor

Dr. Muhammad Imran

A thesis submitted in conformity with the requirements for the degree of *Master of Science* in Electrical (Telecommunication) Engineering

Department of Electrical Engineering

Military College of Signals (MCS)

National University of Sciences and Technology (NUST)

Islamabad, Pakistan

August 2020

Declaration

I, *Muhammad Qasim* declare that this thesis titled "Uplink Interference Management for HetNets Stressed by Uniformly Distributed Wide-Band Jammer" and the work presented in it are my own and has been generated by me as a result of my own original research.

I confirm that:

1. This work was done wholly or mainly while in candidature for a Master of Science degree at NUST
2. Where any part of this thesis has previously been submitted for a degree or any other qualification at NUST or any other institution, this has been clearly stated
3. Where I have consulted the published work of others, this is always clearly attributed
4. Where I have quoted from the work of others, the source is always given. With the exception of such quotations, this thesis is entirely my own work
5. I have acknowledged all main sources of help
6. Where the thesis is based on work done by myself jointly with others, I have made clear exactly what was done by others and what I have contributed myself

_____

Muhammad Qasim,

00000280973

Copyright Notice

Abstract

Intentional jammers (IJs) can be used by the attackers for launching of distributed denial of service attacks in 5G cellular networks. These adversaries are assumed to have adequate information about the network specifications, such as duration, transmit power and positions. With these assumptions, the IJs gain the ability to disrupt the legitimate communication of the network. Heterogeneous cellular networks (HetNets) can be considered a vital enabler for 5G cellular networks. Small base stations (SBSs) are deployed inside macro base station (MBS) in order to improve spectral efficiency and capacity. Due to orthogonal frequency division multiplexing assumption, HetNets' performance is mainly limited by inter-cell interference (ICI). Additionally, there exist IJs-interference (IJs-I), which significantly degrades the network coverage depending on the IJs' transmit power levels and their proximity with the target. The proposed work explores the uplink (UL) coverage performance of HetNets in presence of both IJs-I and ICI. Moreover, in order to reduce the effects of ICI and IJs-I, reverse frequency allocation (RFA) is employed which is a proactive interference abating scheme. In RFA, different sub-bands of available spectrum are utilized by MBS and SBS in alternate regions. In the proposed setup bottlenecks in the UL coverage has been investigated in the presence of IJ in HetNets. Moreover, RFA is employed to mitigate ICI and IJs-I. The setup is evaluated both analytically as well as with the help of simulation. The results demonstrate considerable UL coverage performance improvement by effectively mitigating IJs-I and ICI.

Contents

List of Figures

List of Abbreviations

IJs	Intentional jammers
HetNets	Heterogeneous cellular networks
SBSs	Small base stations
MBS	Macro base station
IJs-I	IJs-interference
UL	Uplink
RFA	Reverse frequency allocation
IoT	Internet of Things
ICI	Inter-cell interference
OFDMA	Orthogonal frequency division multiple access
DDoS	Distributed denial-of-service
NU-HetNets	Non-uniform HetNets
IHPPPs	Independent homogeneous Poisson point processes
FFR	Fractional frequency reuse
SFR	Soft frequency reuse
MIMO	Multiple-input and multiple-output
DL	Downlink
SIR	Signal to interference ratio
SNR	Signal to noise ratio

SINR	Signal to interference noise ratio
NOMA	Non-orthogonal multiple access
5G	Fifth-generation
M-EUs	MBS edge-users
LT	Laplace transform
PGFL	Probability generating functional

Chapter 1

Introduction

1.1 Increased Reliance on Wireless Communication

Today, wireless communication has transformed our lives. In past decade, our reliance on wireless communication has increased many folds[1, 2]. It has made our lives easier due to its usefulness and effectiveness. Social networks and video streaming applications have increased our reliance on smart phones that leads to increased traffic load on cellular networks. Exponentially growing demand for high data rates and ubiquitous coverage requires the wireless network providers to boost both network's capacity and coverage.

In recent times, data usage has grown about 200 percent and, thus, leverages Internet of Things (IoT) in Heterogeneous cellular networks (HetNets) [1–3]. IoT is an organization of inter connected computing devices capable of transferring data without requiring human to computer interaction. IoT technology can be used in smart homes, elder care, medical care, transportation, agriculture etc. As a result, the network operators are now looking for more flexible and advanced network topologies, to satisfy user demands [2].

1.2 Utilizing HetNets

The traditional homogeneous networks faces great challenges in order to meet the ever increasing demand of data. Therefore, HetNets have to be utilized to cater for the data

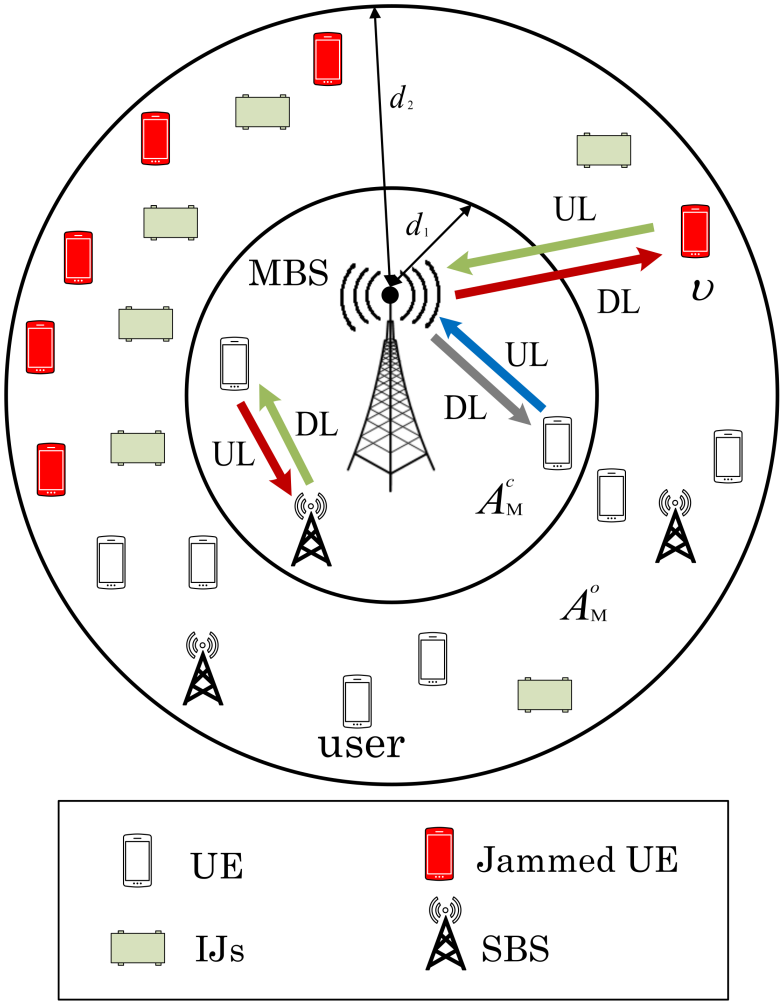

Figure 1.1: HetNet having RFA and IJs in two-tier. MBS, SBSs, users and IJs follow IHPPPs.

requirements. Different wireless access technologies with separate constraints and capabilities are part of HetNets.

For HetNets, coverage, bandwidth quality and performance is improved by implementation of ultra-dense Small base stations (SBSs) within the region served by Macro base station (MBS), as seen in Fig. 1.1 [2, 4].

1.3 OFDMA

Orthogonal frequency division multiple access (OFDMA) provides multiple access by assigning each user a subsets of subcarriers, allowing simultaneous transmission from several users. The usage of OFDMA in HetNets significantly reduces Inter-cell interfer-

ence (ICI) which is a significant limiting factor in improving coverage in Hetnets because it significantly decrease the coverage of MBS edge-users (M-EUs) in HetNets [3].

1.4 DDoS

As the importance of communication in our daily lives is increasing, we are more prone to being target of Distributed denial-of-service (DDoS) attacks which can blackout our communications. DDoS is a rapidly growing problem. The multitude and variety of both the attacks and the defense approaches is overwhelming [5]. Low transmit power levels of user in uplink (UL) communications renders it more prone to DDoS attacks [6], [7]. Therefore, this work investigate Intentional jammers (IJs) attacks to reduce target's UL Signal Interference Ratio (SIR) [8].

1.5 IJs'

Generally, IJs' attacks the public attractions places in MBS coverage area to reduce network coverage. The IJs try to degrade the UL communications by adding significant IJs-interference (IJs-I) in the communication system [9, 10]. However, the transmit power of IJs are limited due to their wide band nature and distance to the target [9]. Hence, for the IJs to be effective, they are required to be deployed near the target in sufficient number and in close proximity [11]. Moreover, this work consider that the IJs possesses necessary details about network parameters including location of target, transmit power and frequency band, thus, forcing the target out of coverage [9, 12, 13].

1.6 ICI

Independent homogeneous Poisson point processes (IHPPPs) are widely used to distribute MBSs, SBSs and users in HetNets due to tractability and ease of analysis [2–4]. In HetNets, OFDMA employment give rise to no/limited ICI, however, ICI remains the main performance limiting attribute [14, 15]. In Non-uniform HetNets (NU-HetNets), users and MBSs are deployed via IHPPP while distribution of SBSs is through Poisson hole process. NU-HetNets lead to lower ICI and thus improves the performance of network coverage [16, 17].

1.7 Interference Reduction Systems

Research has been carried out on different interference reduction systems such as Fractional frequency reuse (FFR) [18] and Soft frequency reuse (SFR) [19]. The SFR system achieves higher spectral efficiency due to frequency reuse, and FFR contributes to reduced interference because of partitioning [20] of the overall usable bandwidth. Reverse frequency allocation (RFA) [14, 19] is another proactive resource management system which helps in reducing interference. Through RFA the maximum bandwidth is made usable in a cell for both MBS and SBS. Consequently, spectral efficiency of RFA is more than SFR and FFR.

1.8 Proposed Work

In this work, RFA will be used in HetNets to abate ICI and IJs-I and, thus, improve UL coverage performance in HetNets. The proposed network setup promises higher network capacity by effectively reducing ICI and IJs-I in HetNets.

1.9 Research Objectives

The research objectives that can be obtained from the proposed work are given below.

1. Investigation of the disruption caused by IJs' attacks to the legitimate UL communication in HetNets.
2. The mitigation of both ICI and IJs-I for the improvement of network performance gain. For this, among the best available techniques such as RFA is employed.
3. This work focuses on increasing capacity and coverage of the network and, thus, renders HetNets as a key enabler for future 5G.
4. To make the network more resilient to both ICI and IJs-I. This can be achieved by efficient resource utilization via RFA.
5. To investigate UL coverage for the proposed setup against different network parameters, such as SBS density, IJs' density, and SIR threshold.

1.10 Thesis Organization

Chapter 1 introduces problem context and outline of the thesis. Chapter 2 provides the literature review of various stages and different aspects of thesis, which includes understanding the research problem and some key concepts. Chapter 3 discusses the system model used in proposed work. In chapter 4, Coverage Probability for UL has been discussed. Chapter 5 presents and compares the detailed experimental results and discussion, followed by the conclusion and future prospects of the project.

Chapter 2

Literature Review

2.1 Jamming

Coverage holes can be created in the network by blocking of electromagnetic waves from reaching the receiver [12]. Sufficient knowledge of network parameters is essential from jamming the communication. Different types of jamming attacks are studied by the authors in [21]. These include, wide-band jammers, noise jammers, partial band jammers, equalization jamming, and automatic gain control jamming. Additionally, the work investigates different jamming attack techniques and various types of targets. They conclude that advanced and sophisticated jamming techniques are required to jam the more complex wireless systems.

In [22], deep recurrent and deep convolutional neural networks are used for detecting the jamming attacks. OFDMA based signaling implemented on software defined radios is used to determine the type and presence of jammer in the network. Their proposed model leads to 85% accuracy in jamming detection and classification.

In [23], Multiple-input and multiple-output (MIMO) networks have been probed by authors in the presence of advanced jamming attacks from jammers having the capability to change the jamming energy. A detailed comparison of different jamming schemes utilized in MIMO networks has also been carried out. Their proposed model assumes that the jammers can increase their transmit power levels to cause severe network performance degradation. Moreover, they investigate different jamming attack scenarios in

MIMO networks and their effectiveness.

In [24] authors have designed an advanced receiver that effectively mitigates the effects of jamming on UL system of massive MIMO networks. The authors have assumed the degrading property of jammers in both pilot and data transmission phases. Their proposed scheme estimates the jamming channel along with the legitimate channel in the pilot phase, which is then used for building filters that neutralize jamming effects on the receiver.

2.2 Anti Jamming

A survey of various jamming and anti jamming techniques has been carried out in [25]. The authors analyzes different types of jammers alongwith strategy for placing the jammers in order for it to be more effective. The effects of various jamming attacks are different on the target. For example, all the available resources are utilized by constant jammers and it jams the network without any break. Whereas, a reactive jammer is more suitable for a network having resource constraint as it attacks the target only when a specific condition is met. It is difficult to detect a jammer with low power, however, a high power jammer will be easily detected but will be able to jam most of the network. Location of jammer also plays an important role in enhancing the effects of jamming. Anti jamming techniques can significantly reduce the effect of jammers. There are various ways to reduce the effects of jammers such as moving from jammed channel to a non jammed channel or moving from jammed area to non jammed area. Detecting presence of jammers is easy but detecting the type of jammer is difficult. Anti jamming for a mobile nodes is difficult as compared to static nodes.

Hybrid automatic repeat request in layer 2 has been introduced in [26] alongwith single input multiple output anti jamming technique in layer 1. Authors propose an anti jamming sub-carrier/power allocation scheme for hybrid automatic repeat request based single input multiple output OFDMA in uplink video communication networks. Peak signal to noise ratio improved by over 11 dB using the proposed scheme. Peak signal to noise ratio was further improved by around 2 dB with addition of hybrid automatic repeat request.

2.3 RFA

RFA scheme is a technique which ensures inter cell orthogonality by splitting up the cell in multiple spatial regions and optimal allocation of frequencies. RFA improves spectrum sharing, increases the data rate and reduces interference from MBS. For the RFA employment in HetNets, two non-overlapping regions have been formed from coverage region of MBS, consisting of inner, A_k^c, and outer region, A_k^o, $\forall k \in \{\text{M, S}\}$ [14, 27].

The authors in [14], use RFA and load balancing to mitigate ICI. Their results indicate significant coverage performance improvement for MBS edge user by using their proposed setup. In [28], variants of RFA are proposed to improve network coverage performance.The authors have also developed a hybrid RFA scheme which combines advantages of various schemes. Through results, the authors show that the variants of RFA lead to significant coverage improvement due to effective resource utilization.

2.4 HetNets

In order to improve capacity and network coverage in HetNets, coverage region of MBS consists of multiple SBSs. However, the introduction of multiple BSs results in enhanced interference and complications, making the analysis and simulation difficult. In [29], the author has divided HetNets in closed and open access networks. In closed access networks, the access of user is limited to particular tier/BS, whereas in open access networks, users have access to all BS in complete network. The author has also discussed use of massive MIMO in HetNets and homogeneous systems.

Fixed cell size MIMO HetNets were modeled in [30] alongwith comparison of single and multi tier networks. However, fixed distances were assumed for association of a user with the BS which is not practical.

Zero force precoding in HetNets consisting of multi antenna has been discussed in [31]. Comparison between open and closed access has been carried out using rate per user and coverage probability. The performance of system has also been calculated using various multiple antenna techniques.

Mitigation of interference in uplink channel of HetNets have been catered for in [32] by controlling power and specified resource allocation for every user. Reduction in interference was observed by use of semi orthogonal allocation scheme and improvement in system capacity was noticed by optimal power allocation.

In [33], authors have formed a HetNet by use of one MBS and multiple SBSs having antennas of large scale employing hybrid digital and analog beam forming. Near optimal results were obtained by use of only four RF chains. Moreover, the computational complexity was also significantly reduced.

In [34], authors evaluates the performance of adaptable controlled cell range expansion technique in HetNet with enhanced ICI coordination scheme. Comparison of the proposed technique has been carried out with state of the art techniques. Results show that the adaptable controlled cell range expansion technique can significantly improve user throughput.

In [35], two tier HetNet model with intra tier dependence, where the MBSs follow Poisson point process and the pico base stations follow Matern cluster process have been proposed. Exact expressions for interference and outage probability have been derived based on distance between a user equipment and serving BS. The results indicate that small cells improve per user capacity and area spectral efficiency, however outage is not improved.

2.5 Small Cell Networks

Introduction of multiple BSs in Hetnets results in increased interference. Performance of the network having small cells, can be improved by considering parameters such as interference, size of cell, UL power control and deployment strategy [36]. In small cells, power of user equipment is a significant contributing factor in interference. Authors in [36] have shown that 18 dBm power of user equipment in uniformly distributed small cells produced better results than 23 dBm.

2.6 Multi-Slope Path Loss Model

The benefits of HetNets can be realized by offloading the traffic towards small cells [37]. Generally single slope path loss model is being used for user association. The accuracy of single slope path loss model is less because of increasing density of networks and asymmetrical patterns of the cell. Authors in this paper have considered a model of laying pico cells over macro cells in down link HetNets and proposed use of dual slope path loss model. Results indicate that performance of the system is improved by using dual slope path loss model as more traffic is offloaded from macro to pico cells.

Use of single path loss model can produce inaccuracies in received and interference powers as compared to true values. In [38], authors have discussed multi slope path loss model which has varying path loss exponent for varying distance range. The expressions for SIR, signal to noise ratio (SNR) and signal to interference noise ratio (SINR) have been derived. Derivations indicate that the SIR decreases with network density, however SNR increases with network density. Moreover, maximum value of SINR is achieved at particular finite density.

2.7 Interference management

Soft frequency reuse technique can be used to improve interference management [39]. Authors have shown numerically in this paper that soft frequency reuse can perform better than frequency resource partitioning technique in any load condition. Average user rate can also be improved by soft frequency reuse.

Interference can be reduced by use of fractional frequency reuse technique because of its bandwidth efficiency and OFDMA suitability for cellular networks [40]. Authors also compare fractional frequency reuse and soft frequency reuse techniques. Results indicate that performance of fractional frequency reuse is better than soft frequency reuse in signal to interference noise ratio and rate coverage probability, however, soft frequency reuse provides better spectral efficiency.

2.8 NU-HetNets

NU-HetNets along with SFR is investigated in [19]. The coverage probability expressions has been derived by the authors while assuming both U-HetNets and NU-HetNets. Their outcomes suggest that NU-HetNets along with SFR results in significant coverage improvement due to effective ICI mitigation.

In [41], a novel technique for SBS deployment is proposed, where the SBSs are powered on via renewable energy source. The authors termed this approach as off-grid NU-HetNets, where the SBS are not grid connected. Moreover, HetNets' performance is evaluated by considering off-grid SBSs and on-grid MBSs. They derive expressions for coverage probability, association probabilities, and distance distribution while considering the proposed setup. Their results indicate that off-grid SBSs provide lower coverage due to limited available power.

NU-HetNets with Non-orthogonal multiple access (NOMA) is investigated in [17]. The work evaluates energy efficiency and Downlink (DL) coverage for the proposed model. Results show that employment of NOMA leads to higher rate coverage and energy efficiency in HetNets.

Similarly, NU-HetNet in conjunction with RFA is considered in [42]. In this work, SBSs are assumed to be muted near MBS to avoid significant co-tier interference. However, SBSs are kept active in MBS edge area to improve edge users' coverage. Moreover, the authors characterize both rate and coverage analyses for the proposed setup. The results show that NU-HetNets in MBS coverage edge area improve the network coverage and rate.

2.9 Thesis proposal

This proposal differs from the state-of-the-art in following ways:

1. Works in [21–23] explore different jamming attacks in different network types, however, they lack the evaluation of IJs in HetNets. Therefore, in this work, the IJs in HetNets are investigated.

2. The works in [14, 17, 19, 27, 28, 41, 42] investigate the mitigation of ICI by RFA in HetNets. However, they lack the utilization of RFA to abate IJs-I. Therefore, in this work, RFA is employed to mitigate both ICI and IJs-I.

3. In [17, 28, 42], DL coverage analysis is performed, while the focus of this work is on analyzing the bottleneck UL coverage analysis of the MBS edge user.

Chapter 3

System Model

Network layout along with the interference mitigation schemes used in proposed research has been introduced in this chapter. Moreover, network assumptions, IJs' attack mechanism and RFA are discussed here. Furthermore, mathematical preliminaries obtained here are also utilized in Chapter 4 for coverage probabilities derivation.

3.1 Network Layout and Assumptions

HetNet model having two tiers is considered, which includes MBSs, SBSs, user, and IJs. MBSs, SBSs, users, and IJs are distributes via IHPPPs with densities ρ_{M}, ρ_{S}, ρ_u and ρ_{J}, respectively. The UL communication is restricted with a help of cluster of IJs which severely effect UL communication. It is assumed that the parameters of the network are known to the attackers so the UL communication can be targeted. IJs are transmitting unwanted energies in the legitimate communication band and, thus, degrade the network performance. Single cluster of IJs is assumed to be around the target area which can have significant jamming effect on the network. Moreover, only intra cluster IJs-I has been examined which can simplify the analysis.

To mitigate ICI and IJs-I, a proactive interference abating scheme, i.e., RFA is employed. A typical user has been considered for analysis. β denotes the path loss exponents while $|h|$ denotes Rayleigh fading gain. In [43], author has modeled a HetNet system consisting of two tiers having one MBS and multiple SBSs which are distributed according to Poisson point process. Moreover, the association of users carried out via maximum

received power scheme [43].

The effect of noise in the network has been neglected and only the effect of interference has been considered.

3.2 IJs Mechanism

IJs transmit noise energy to reduce network coverage by targeting the legitimate communications [21]. The coverage in the network is reduced by IJs with IJs-I. In addition, we consider IJs to be low-cost and lightweight transmitters which are deployed randomly via IHPPP throughout the MBS coverage region. Severe degradation is experienced in M-EUs UL communication because of ICI and M-EUs enhanced distance from the MBS. Desired communication frequency can be jammed by IJs.

Because of its wide-band existence, the noise power may be negligible and does hardly any harm in the presence of few IJs present. Considerable IJs-I is achieved as the density and power of the IJs increases, and thus degrades the network's performance [8, 22]. More precisely, by increasing density of IJs and transmission capacity, UL contact of M-EUs in HetNets can be completely blocked.

3.3 Reverse Frequency Allocation

High throughput is achieved in HetNet with the help of frequency reuse leading to increase in ICI. However, in order to enhance spectral efficiency of the network two varying sub bands are being used for DL and UL communication. RFA-based network partitioning eliminates interference and increases coverage, because no fixed spectrum allocation is assigned to SBS. Therefore, employment of RFA can make the entire spectrum of MBS available to SBSs in non-overlapping regions and reverse direction.

As shown in Fig. 3.1, sub-bands used in SBSs and MBSs for RFA are in reverse order for $A_l^g \ \forall \ l \in (\mathrm{M}, \mathrm{S})$ and $g \in (c, o)$.

In RFA, allotted frequency, F, is subdivided into two sub-bands, F_1 and F_2, such that

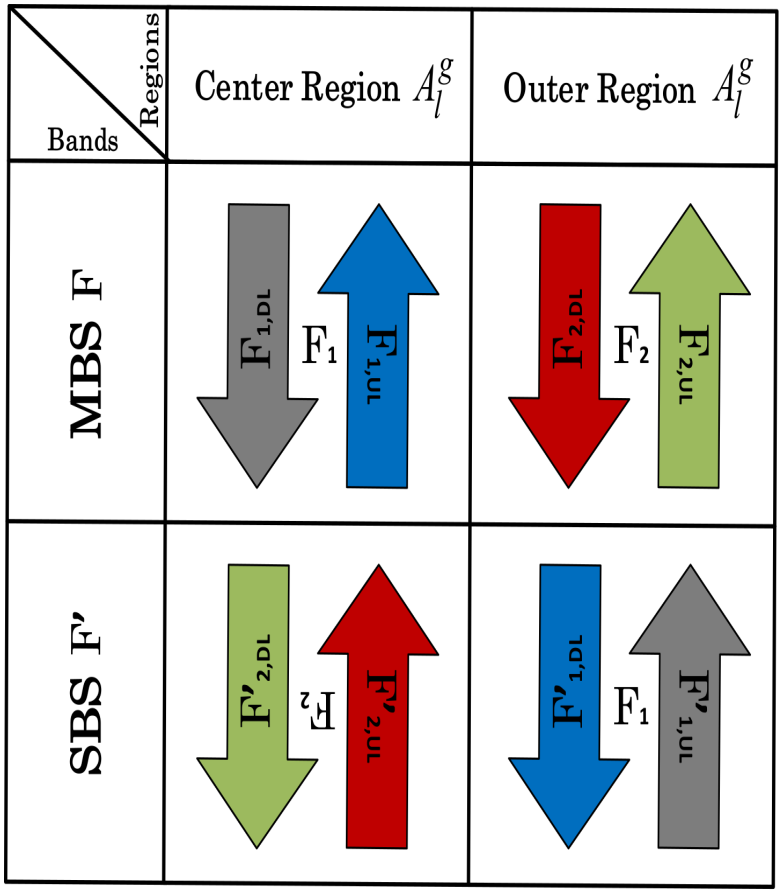

Figure 3.1: Two-tier HetNet model with RFA.

$\mathrm{F} = \bigcup_{z\in(1,2)} \mathrm{F}z$, as shown in Fig. 3.1. Here, F_1 and F_2 represent MBS bands to be utilized respectively in A_{M}^o and A_{M}^c. Sub-bands F1and F2 are further divided into sub-carriers DL and UL, and are modeled as $\mathrm{F}_1 = \mathrm{F}_{1,\mathrm{DL}} + \mathrm{F}_{1,\mathrm{UL}}$ and $\mathrm{F}_2 = \mathrm{F}_{2,\mathrm{DL}} + \mathrm{F}_{2,\mathrm{UL}}$, respectively. The sub-bands of MBS, F_1 and F_2, are used as frequency sub-bands, F'_1 and F'_2, for SBS but in reverse direction and in alternate regions, i.e., outer region of SBS, A_{S}^o, and center region of SBS, A_{S}^c. For SBS, F'_1 and F'_2, bands are split into DL and UL sub-carriers and are specified as $\mathrm{F}'_2 = \mathrm{F}'_{2,\mathrm{DL}} + \mathrm{F}'_{2,\mathrm{UL}}$ and $\mathrm{F}'_1 = \mathrm{F}'_{1,\mathrm{DL}} + \mathrm{F}'_{1,\mathrm{UL}}$, respectively.

Chapter 4

Proposed Technique

4.1 Coverage Probability for UL in presence of IJs without RFA

In HetNet, it is presumed that in order to degrade the M-EUs' UL communication, IJs are deployed uniformly around the MBS coverage area using IHPPP. Therefore, in such a network environment IJs-I and ICI are the main efficiency limiting factors. The expression for UL coverage probability, $P^{\mathrm{UL}}_{A^c_{\mathrm{M}}}(\Gamma_{\mathrm{M}})$, for MBS associated ν in A^c_{M} with IJs without RFA may be expressed as

$$P^{\mathrm{UL}}_{A^c_{\mathrm{M}}}(\Gamma_{\mathrm{M}}) = P\left(\mathrm{SIR}^{\mathrm{UL}}_{\mathrm{M}} > \Gamma_{\mathrm{M}}\right). \tag{4.1.1}$$

Here, Γ_{M} is the UL SIR threshold, while $\mathrm{SIR}^{\mathrm{UL}}_{\mathrm{M}}$ indicates the received UL SIR. $\mathrm{SIR}^{\mathrm{UL}}_{\mathrm{M}}$ from (4.1.1) can be written as

$$\mathrm{SIR}^{\mathrm{UL}}_{\mathrm{M}} = \frac{P^{\mathrm{UL}}_{t,\nu}|h_{\mathrm{M}}|^2 r_{\mathrm{M}}^{-\beta}}{I_{\mathrm{M},A} + I_{\mathrm{S},A} + I_{J,A}},$$

$$= \frac{P^{\mathrm{UL}}_{t,\nu}|h_{\mathrm{M}}|^2 r_{\mathrm{M}}^{-\beta}}{\sum\limits_{l\in\phi_{\mathrm{M}}} P_{t,l}|h_l|^2 r_l^{-\beta} + \sum\limits_{k\in\phi_{\mathrm{S}}} P_{t,k}|h_k|^2 r_k^{-\beta} + \sum\limits_{j\in\phi_J} P_{t,j}|h_j|^2 r_j^{-\beta}}. \tag{4.1.2}$$

In (4.1.2), the UL interference in A_{M}^{c} is the accumulative interference's from i) MBS-tier, $I_{\mathrm{M},A}$, ii) SBS-tier, $I_{\mathrm{S},A}$, and iii) IJs, $I_{J,A}$. $r_{()}^{-\beta}$ indicates the distance from IJs or BS. Moreover, $P_{t,\nu}^{\mathrm{UL}}$ is the transmit power in UL. $P_{t,l}, P_{t,k}$ and $P_{t,j}$ represent transmit powers of MBS, SBS and IJs, respectively. ϕ_{M}, ϕ_{S} and ϕ_{J} are the IHPPPs of MBSs, SBSs and IJs, respectively. Moreover, A represents MBS coverage area, i.e., $A = A_{\mathrm{M}}^{c} \bigcup A_{\mathrm{M}}^{o}$. Using (4.1.2), (4.1.1) can be written as

$$
\begin{aligned}
P_{A_{\mathrm{M}}^{c}}^{\mathrm{UL}}(\Gamma_{\mathrm{M}}) &= P\left(\frac{P_{t,\nu}^{\mathrm{UL}}|h_{\mathrm{M}}|^{2} r_{\mathrm{M}}^{-\beta}}{I_{\mathrm{M},A} + I_{\mathrm{S},A} + I_{J,A}} > \Gamma_{\mathrm{M}}\right) \\
&= \mathrm{E}_{r_{\mathrm{M}}, I_{\mathrm{M},A}, I_{\mathrm{S},A}, I_{J,A}}\left[\exp\left(-\frac{r_{\mathrm{M}}^{\beta}\Gamma_{\mathrm{M}}}{P_{t,\nu}^{\mathrm{UL}}}(I_{\mathrm{M},A} + I_{\mathrm{S},A} + I_{J,A})\right)\right] \\
&= \mathrm{E}_{r_{\mathrm{M}}}\left[\mathcal{L}_{I_{\mathrm{M},A}}(s) \times \mathcal{L}_{I_{\mathrm{S},A}}(s) \times \mathcal{L}_{I_{J,A}}(s)\right]\Big|_{s=\frac{r_{\mathrm{M}}^{\beta}\Gamma_{\mathrm{M}}}{P_{t,\nu}^{\mathrm{UL}}}}.
\end{aligned} \tag{4.1.3}
$$

Here, $\mathcal{L}_{I_{\mathrm{M},A}}(s), \mathcal{L}_{I_{\mathrm{S},A}}(s),$ and $\mathcal{L}_{I_{J,A}}(s)$ denote the Laplace transform (LT) of $I_{\mathrm{M},A}$, $I_{\mathrm{S},A}$, and $I_{J,A}$, respectively. Moreover, $\mathrm{E}[\cdot]$ denotes the expectation of LTs.
The LT of MBS-tier interference , $\mathcal{L}_{I_{\mathrm{M},A}}(s)$, in A, can be written as

$$
\begin{aligned}
&\mathcal{L}_{I_{\mathrm{M},A}}(s) = \\
&\exp\left(\frac{\rho_{\mathrm{M}}\pi\gamma_{\circ}\Gamma_{\mathrm{M}} d_{2}^{(2-\beta)} r_{\mathrm{M}}^{\beta}}{\beta/2-1} {}_2F_1\left(1, 1-\frac{2}{\beta}, 2-\frac{2}{\beta}, -\gamma_{\circ}\Gamma_{\mathrm{M}}\left(\frac{r_{\mathrm{M}}}{d_2}\right)^{\beta}\right) - \right. \\
&\left.\frac{\rho_{\mathrm{M}}\pi\gamma_{\circ}\Gamma_{\mathrm{M}} y^{(2-\beta)} r_{\mathrm{M}}^{\beta}}{\beta/2-1} {}_2F_1\left(1, 1-\frac{2}{\beta}, 2-\frac{2}{\beta}, -\gamma_{\circ}\Gamma_{\mathrm{M}}\left(\frac{r_{\mathrm{M}}}{y}\right)^{\beta}\right)\right).
\end{aligned} \tag{4.1.4}
$$

Proof: See Appendix A.1 for the proof of (4.1.4). In (4.1.4), $\gamma_{\circ}$ is the ratio of $P_{t,\mathrm{M}}$ and $P_{t,\nu}^{\mathrm{UL}}$, where $P_{t,\mathrm{M}}$ is transmission power of MBS-tier.

Similar to approached used in (4.1.4), the LT of the received interference from SBS-tier, $\mathcal{L}_{I_{\mathrm{S},A}}(s)$, in A, can be written as

$$\mathcal{L}_{I_{\mathrm{S},A}}(s) =$$

$$\exp\left(\frac{\rho_{\mathrm{S}}\pi\gamma_1\Gamma_{\mathrm{M}}x_2^{(2-\beta)}r_{\mathrm{M}}^{\beta}}{\beta/2-1}{}_2F_1\left(1,1-\frac{2}{\beta},2-\frac{2}{\beta},-\gamma_1\Gamma_{\mathrm{M}}\left(\frac{r_{\mathrm{M}}}{x_2}\right)^{\beta}\right)-\right.$$

$$\left.\frac{\rho_{\mathrm{S}}\pi\gamma_1\Gamma_{\mathrm{M}}x_1^{(2-\beta)}r_{\mathrm{M}}^{\beta}}{\beta/2-1}{}_2F_1\left(1,1-\frac{2}{\beta},2-\frac{2}{\beta},-\gamma_1\Gamma_{\mathrm{M}}\left(\frac{r_{\mathrm{M}}}{x_1}\right)^{\beta}\right)\right). \tag{4.1.5}$$

Here, γ_1 is ratio of $P_{t,\mathrm{S}}$ and $P_{t,\nu}^{\mathrm{UL}}$, where $P_{t,\mathrm{S}}$ is the transmit power of SBS.
Similar to approached used in (4.1.4), the LT of the interference received from IJs, $\mathcal{L}_{I_J,A}(s)$, in A, can be given as

$$\mathcal{L}_{I_{J,A}}(s) =$$

$$\exp\left(\frac{\rho_J\pi\gamma_2\Gamma_{\mathrm{M}}z_2^{(2-\beta)}r_{\mathrm{M}}^{\beta}}{\beta/2-1}{}_2F_1\left(1,1-\frac{2}{\beta},2-\frac{2}{\beta},-\gamma_2\Gamma_{\mathrm{M}}\left(\frac{r_{\mathrm{M}}}{z_2}\right)^{\beta}\right)-\right.$$

$$\left.\frac{\rho_J\pi\gamma_2\Gamma_{\mathrm{M}}z_1^{(2-\beta)}r_{\mathrm{M}}^{\beta}}{\beta/2-1}{}_2F_1\left(1,1-\frac{2}{\beta},2-\frac{2}{\beta},-\gamma_2\Gamma_{\mathrm{M}}\left(\frac{r_{\mathrm{M}}}{z_1}\right)^{\beta}\right)\right). \tag{4.1.6}$$

Here, γ_2 is the ratio of $P_{t,J}$ and $P_{t,\nu}^{\mathrm{UL}}$ where $P_{t,J}$ is the transmit power of IJs and z_1 and z_2 define the effective attacking areas of the jammers, s.t., $z_1 \leq z_2$.
ν is located in A_{M}^{c} or in A_{M}^{o} (denoted as $\nu_{A_{\mathrm{M}}^{c}}$ and $\nu_{A_{\mathrm{M}}^{o}}$, respectively), while associated with MBS at a distance $r_{\mathrm{M},\nu}$, has PDFs of distances given, respectively, as (4.1.7) and (4.1.8) [44] [45]

$$f_{r_{\mathrm{M}}|\nu_{A_{\mathrm{M}}^{c}}}(r_{\mathrm{M}}) = \frac{2\pi\rho_{\mathrm{M}}r_{\mathrm{M}}\exp(-\rho_{\mathrm{M}}\pi r_{\mathrm{M}}^2)}{1-\exp\left(-\rho_{\mathrm{M}}\pi d_1^2\right)}, \tag{4.1.7}$$

and

$$f_{r_{\mathrm{M}}|\nu_{A_{\mathrm{M}}^{o}}}(r_{\mathrm{M}}) = \frac{2\pi\rho_{\mathrm{M}}r_{\mathrm{M}}\exp(-\rho_{\mathrm{M}}\pi r_{\mathrm{M}}^2)}{\exp\left(-\rho_{\mathrm{M}}\pi d_1^2\right)}. \tag{4.1.8}$$

UL coverage probability expression, $P^{\mathrm{UL}}_{A^c_{\mathrm{M}}}(\Gamma_{\mathrm{M}})$, having uniformly deployed IJs without RFA for MBS associated ν in A^c_{M}, may be achieved as

$$P^{\mathrm{UL}}_{A^c_{\mathrm{M}}}(\Gamma_{\mathrm{M}}) = \int_{y}^{d_1} \mathcal{L}_{I_{\mathrm{M},A}}(s) \times \mathcal{L}_{I_{\mathrm{S},A}}(s) \times \mathcal{L}_{I_{J,A}}(s)\, f_{r_{\mathrm{M},\nu}|\nu_{A^c_{\mathrm{M}}}}(r_{\mathrm{M},\nu})\, dr_{\mathrm{M},\nu}. \tag{4.1.9}$$

By substituting (4.1.4), (4.1.5), (4.1.6) and (4.1.7) into (4.1.9), $P^{\mathrm{UL}}_{A^c_{\mathrm{M}}}(\Gamma_{\mathrm{M}})$ is achieved as (4.1.11).

Similarly, for uniformly distributed IJs without RFA, UL coverage probability expression, $P^{\mathrm{UL}}_{A^o_{\mathrm{M}}}(\Gamma_{\mathrm{M}})$, for MBS associated ν in A^o_{M} can be written as

$$P^{\mathrm{UL}}_{A^o_{\mathrm{M}}}(\Gamma_{\mathrm{M}}) = \int_{d_1}^{d_2} \mathcal{L}_{I_{\mathrm{M},A}}(s) \times \mathcal{L}_{I_{\mathrm{S},A}}(s) \times \mathcal{L}_{I_{J,A}}(s)\, f_{r_{\mathrm{M},\nu}|\nu_{A^o_{\mathrm{M}}}}(r_{\mathrm{M},\nu})\, dr_{\mathrm{M},\nu}. \tag{4.1.10}$$

By putting (4.1.4), (4.1.5), (4.1.6) and (4.1.8) in (4.1.10), $P^{\mathrm{UL}}_{A^o_{\mathrm{M}}}(\Gamma_{\mathrm{M}})$ is written as (4.1.12).

4.2 Coverage Probability for UL in presence of IJs with RFA

The expression for UL coverage probability, $P^{\mathrm{UL},*}_{A^c_{\mathrm{M}}}(\Gamma_{\mathrm{M}})$, with IJs and RFA while considering ν in A^c_{M} can be expressed as

$$P^{\mathrm{UL},*}_{A^c_{\mathrm{M}}}(\Gamma_{\mathrm{M}}) = P\left(\mathrm{SIR}^{\mathrm{UL}}_{\mathrm{M}} > \Gamma_{\mathrm{M}}\right). \tag{4.2.1}$$

The UL interference experienced while employing RFA, is the aggregate of MBS-tier UL interference in A^c_{M}, i.e., $I^{\mathrm{UL}}_{\phi_{\mathrm{M}},A^c_{\mathrm{M}}}$, SBS-tier DL interference in A^o_{M}, i.e., $I^{\mathrm{DL}}_{\phi_i,A^o_{\mathrm{M}}}$, and interference from IJs, i.e., $I_{J,A}$. Therefore, $\mathrm{SIR}^{\mathrm{UL}}_{\mathrm{M}}$ from (4.2.1) can be written as

$$\mathrm{SIR}^{\mathrm{UL}}_{\mathrm{M}} = \frac{P^{\mathrm{UL}}_{t,\nu}|h_{\mathrm{M}}|^2 r_{\mathrm{M}}^{-\beta}}{I^{\mathrm{UL}}_{\phi_{\mathrm{M}},A^c_{\mathrm{M}}} + I^{\mathrm{DL}}_{\phi_{\mathrm{S}},A^o_{\mathrm{M}}} + I_{J,A}}. \tag{4.2.2}$$

$$P^{\mathrm{UL}}_{A^c_{\mathrm{M}}}(\Gamma_{\mathrm{M}}) = \frac{2\pi\rho_{\mathrm{M}}}{1-\exp(-\rho_{\mathrm{M}}\pi d_1^2)}\exp\left(\frac{\pi\Gamma_{\mathrm{M}} r_{\mathrm{M}}^{\beta}}{\beta/2-1}\left[\rho_{\mathrm{M}}\gamma_{\circ} d_2^{(2-\beta)}\mathcal{J}\left(\beta,-\Gamma_{\mathrm{M}}\gamma_{\circ}\left(\frac{r_{\mathrm{M}}}{d_2}\right)^{\beta}\right)-\rho_{\mathrm{M}}\gamma_{\circ} y^{(2-\beta)}\mathcal{J}\left(\beta,-\Gamma_{\mathrm{M}}\gamma_{\circ}\left(\frac{r_{\mathrm{M}}}{y}\right)^{\beta}\right)+\right.\right.$$

$$\rho_{\mathrm{S}}\gamma_1 x_2^{(2-\beta)}\mathcal{J}\left(\beta,-\Gamma_{\mathrm{M}}\gamma_1\left(\frac{r_{\mathrm{M}}}{x_2}\right)^{\beta}\right)-\rho_{\mathrm{S}}\gamma_1 x_1^{(2-\beta)}\mathcal{J}\left(\beta,-\Gamma_{\mathrm{M}}\gamma_1\left(\frac{r_{\mathrm{M}}}{x_1}\right)^{\beta}\right)+\rho_J\gamma_2 z_2^{(2-\beta)}\mathcal{J}\left(\beta,-\Gamma_{\mathrm{M}}\gamma_2\left(\frac{r_{\mathrm{M}}}{z_2}\right)^{\beta}\right)-$$

$$\left.\left.\rho_J\gamma_2 z_1^{(2-\beta)}\mathcal{J}\left(\beta,-\Gamma_{\mathrm{M}}\gamma_2\left(\frac{r_{\mathrm{M}}}{z_1}\right)^{\beta}\right)\right]-\rho_{\mathrm{M}}\pi r_{\mathrm{M}}^2\right) r_{\mathrm{M}} dr_{\mathrm{M}}. \tag{4.1.11}$$

$$P^{\mathrm{UL}}_{A^o_{\mathrm{M}}}(\Gamma_{\mathrm{M}}) = \frac{2\pi\rho_{\mathrm{M}}}{\exp(-\rho_{\mathrm{M}}\pi d_1^2)}\exp\left(\frac{\pi\Gamma_{\mathrm{M}} r_{\mathrm{M}}^{\beta}}{\beta/2-1}\left[\rho_{\mathrm{M}}\gamma_{\circ} d_2^{(2-\beta)}\mathcal{J}\left(\beta,-\Gamma_{\mathrm{M}}\gamma_{\circ}\left(\frac{r_{\mathrm{M}}}{d_2}\right)^{\beta}\right)-\rho_{\mathrm{M}}\gamma_{\circ} y^{(2-\beta)}\mathcal{J}\left(\beta,-\Gamma_{\mathrm{M}}\gamma_{\circ}\left(\frac{r_{\mathrm{M}}}{y}\right)^{\beta}\right)\right.\right.$$

$$+\rho_{\mathrm{S}}\gamma_1 x_2^{(2-\beta)}\mathcal{J}\left(\beta,-\Gamma_{\mathrm{M}}\gamma_1\left(\frac{r_{\mathrm{M}}}{x_2}\right)^{\beta}\right)-\rho_{\mathrm{S}}\gamma_1 x_1^{(2-\beta)}\mathcal{J}\left(\beta,-\Gamma_{\mathrm{M}}\gamma_1\left(\frac{r_{\mathrm{M}}}{x_1}\right)^{\beta}\right)+\rho_J\gamma_2 z_2^{(2-\beta)}\mathcal{J}\left(\beta,-\Gamma_{\mathrm{M}}\gamma_2\left(\frac{r_{\mathrm{M}}}{z_2}\right)^{\beta}\right)-$$

$$\left.\left.\rho_J\gamma_2 z_1^{(2-\beta)}\mathcal{J}\left(\beta,-\Gamma_{\mathrm{M}}\gamma_2\left(\frac{r_{\mathrm{M}}}{z_1}\right)^{\beta}\right)\right]-\rho_{\mathrm{M}}\pi r_{\mathrm{M}}^2\right) r_{\mathrm{M}} dr_{\mathrm{M}}. \tag{4.1.12}$$

Equation (4.2.2) can be expanded as

$$\mathrm{SIR}^{\mathrm{UL}}_{\mathrm{M}} =$$

$$\frac{P^{\mathrm{UL}}_{t,\nu}|h_{\mathrm{M}}|^2 r_{\mathrm{M}}^{-\beta}}{\sum\limits_{l\in\phi_{\mathrm{M}}} P^{\mathrm{UL}}_{t,l}|h_l|^2 r_l^{-\beta}+\sum\limits_{k\in\phi_{\mathrm{S}}} P^{\mathrm{DL}}_{t,k}|h_k|^2 r_k^{-\beta}+\sum\limits_{j\in\phi_J} P_{t,j}|h_j|^2 r_j^{-\beta}}. \tag{4.2.3}$$

Here, MBS UL transmit power of ν is, $P^{\mathrm{UL}}_{t,l}$, SBS DL transmit power is $P^{\mathrm{DL}}_{t,k}$, and IJs transmit power is $P_{t,j}$. Further more, by putting (4.2.2) in (4.2.1), we get $P^{\mathrm{UL},*}_{A^c_{\mathrm{M}}}(\Gamma_{\mathrm{M}})$ as

$$P^{\mathrm{UL},*}_{A^c_{\mathrm{M}}}(\Gamma_{\mathrm{M}}) = P\left(\frac{P^{\mathrm{UL}}_{t,\nu}|h_{\mathrm{M}}|^2 r_{\mathrm{M}}^{-\beta}}{I^{\mathrm{UL}}_{\phi_{\mathrm{M}},A^c_{\mathrm{M}}} + I^{\mathrm{DL}}_{\phi_{\mathrm{S}},A^o_{\mathrm{M}}} + I_{J,A}} > \Gamma_{\mathrm{M}}\right)$$

$$= \mathrm{E}_{r_{\mathrm{M}},I^{\mathrm{UL}}_{\phi_{\mathrm{M}},A^c_{\mathrm{M}}},I^{\mathrm{DL}}_{\phi_{\mathrm{S}},A^o_{\mathrm{M}}},I_{J,A}}\left[\exp\left(-\frac{r_{\mathrm{M}}^{\beta}\Gamma_{\mathrm{M}}}{P^{\mathrm{UL}}_{t,\nu}}\left(I^{\mathrm{UL}}_{\phi_{\mathrm{M}},A^c_{\mathrm{M}}}+I^{\mathrm{DL}}_{\phi_{\mathrm{S}},A^o_{\mathrm{M}}}+I_{J,A}\right)\right)\right]$$

$$= \mathrm{E}_{r_{\mathrm{M}}}\left[\mathcal{L}_{I^{\mathrm{UL}}_{\phi_{\mathrm{M}},A^c_{\mathrm{M}}}}(s) \times \mathcal{L}_{I^{\mathrm{DL}}_{\phi_{\mathrm{S}},A^o_{\mathrm{M}}}}(s) \times \mathcal{L}_{I_{J,A}}(s)\right]\Big|_{s=\frac{r_{\mathrm{M}}^{\beta}\Gamma_{\mathrm{M}}}{P^{\mathrm{UL}}_{t,\nu}}}. \tag{4.2.4}$$

The LT of MBS UL interference in A^c_{M}, i.e., $\mathcal{L}_{I^{\mathrm{UL}}_{\phi_{\mathrm{M}},A^c_{\mathrm{M}}}}$, can be written as

$$\mathcal{L}_{I^{\mathrm{UL}}_{\phi_{\mathrm{M}},A^c_{\mathrm{M}}}} =$$

$$\exp\left(\frac{\rho_{\mathrm{M}}\pi\Gamma_{\mathrm{M}}d_1^{(2-\beta)}r_{\mathrm{M}}^{\beta}}{\beta/2-1}{}_2F_1\left(1,1-\frac{2}{\beta},2-\frac{2}{\beta},-\Gamma_{\mathrm{M}}\left(\frac{r_{\mathrm{M}}}{d_1}\right)^{\beta}\right) -\right.$$

$$\left.\frac{\rho_{\mathrm{M}}\pi\Gamma_{\mathrm{M}}y^{(2-\beta)}r_{\mathrm{M}}^{\beta}}{\beta/2-1}{}_2F_1\left(1,1-\frac{2}{\beta},2-\frac{2}{\beta},-\Gamma_{\mathrm{M}}\left(\frac{r_{\mathrm{M}}}{y}\right)^{\beta}\right)\right). \tag{4.2.5}$$

Proof: See Appendix A.2 for the proof of (4.2.5).

Moreover, LT of SBS DL interference in A^o_{M}, i.e., $\mathcal{L}_{I^{\mathrm{DL}}_{\phi_{\mathrm{S}},A^o_{\mathrm{M}}}}$, can be written in a way similar to (4.2.5), and is given as

$$\mathcal{L}_{I^{\mathrm{DL}}_{\phi_{\mathrm{S}},A^o_{\mathrm{M}}}} = \mathcal{L}_{I^{\mathrm{DL}}_{\phi_{\mathrm{S}},A^c_{\mathrm{M}}}} =$$

$$\exp\left(\frac{\rho_{\mathrm{S}}'\pi\gamma_3\Gamma_{\mathrm{M}}x_2^{(2-\beta)}r_{\mathrm{M}}^{\beta}}{\beta/2-1}{}_2F_1\left(1,1-\frac{2}{\beta},2-\frac{2}{\beta},-\gamma_3\Gamma_{\mathrm{M}}\left(\frac{r_{\mathrm{M}}}{x_2}\right)^{\beta}\right) -\right.$$

$$\left.\frac{\rho_{\mathrm{S}}'\pi\gamma_3\Gamma_{\mathrm{M}}x_1^{(2-\beta)}r_{\mathrm{M}}^{\beta}}{\beta/2-1}{}_2F_1\left(1,1-\frac{2}{\beta},2-\frac{2}{\beta},-\gamma_3\Gamma_{\mathrm{M}}\left(\frac{r_{\mathrm{M}}}{x_1}\right)^{\beta}\right)\right). \tag{4.2.6}$$

$$P^{\mathrm{UL},*}_{A^c_{\mathrm{M}}}(\Gamma_{\mathrm{M}}) = \frac{2\pi\rho_{\mathrm{M}}}{1-\exp\left(-\rho_{\mathrm{M}}\pi d_1^2\right)}\Big|_y^{d_1} \exp\left(\frac{\pi\Gamma_{\mathrm{M}} r_{\mathrm{M}}^{\beta}}{\beta/2-1}\left[\rho_{\mathrm{M}} d_1^{(2-\beta)}\mathcal{J}\left(\beta,-\Gamma_{\mathrm{M}}\left(\frac{r_{\mathrm{M}}}{d_1}\right)^{\beta}\right)-\rho_{\mathrm{M}} y^{(2-\beta)}\mathcal{J}\left(\beta,-\Gamma_{\mathrm{M}}\left(\frac{r_{\mathrm{M}}}{y}\right)^{\beta}\right)+\right.\right.$$

$$\rho_{\mathrm{S}}'\gamma_3 d_2^{(2-\beta)}\mathcal{J}\left(\beta,-\Gamma_{\mathrm{M}}\gamma_3\left(\frac{r_{\mathrm{M}}}{d_2}\right)^{\beta}\right)-\rho_{\mathrm{S}}'\gamma_3 {d_1}^{(2-\beta)}\mathcal{J}\left(\beta,-\Gamma_{\mathrm{M}}\gamma_3\left(\frac{r_{\mathrm{M}}}{d_1}\right)^{\beta}\right)+\rho_J\gamma_2 d_2^{(2-\beta)}\mathcal{J}\left(\beta,-\Gamma_{\mathrm{M}}\gamma_2\left(\frac{r_{\mathrm{M}}}{d_2}\right)^{\beta}\right)-$$

$$\left.\left.\rho_J\gamma_2 y^{(2-\beta)}\mathcal{J}\left(\beta,-\Gamma_{\mathrm{M}}\gamma_2\left(\frac{r_{\mathrm{M}}}{y}\right)^{\beta}\right)\right]-\rho_{\mathrm{M}}\pi r_{\mathrm{M}}^2\right) r_{\mathrm{M}} dr_{\mathrm{M}}. \tag{4.2.8}$$

$$P^{\mathrm{UL},*}_{A^o_{\mathrm{M}}}(\Gamma_{\mathrm{M}}) = \frac{2\pi\rho_{\mathrm{M}}}{\exp\left(-\rho_{\mathrm{M}}\pi d_1^2\right)}\Big|_{d_1}^{d_2} \exp\left(\frac{\pi\Gamma_{\mathrm{M}} r_{\mathrm{M}}^{\beta}}{\beta/2-1}\left[\rho_{\mathrm{M}} d_2^{(2-\beta)}\mathcal{J}\left(\beta,-\Gamma_{\mathrm{M}}\left(\frac{r_{\mathrm{M}}}{d_2}\right)^{\beta}\right)-\rho_{\mathrm{M}} {d_1}^{(2-\beta)}\mathcal{J}\left(\beta,-\Gamma_{\mathrm{M}}\left(\frac{r_{\mathrm{M}}}{d_1}\right)^{\beta}\right)+\right.\right.$$

$$\rho_{\mathrm{S}}'\gamma_3 d_1^{(2-\beta)}\mathcal{J}\left(\beta,-\Gamma_{\mathrm{M}}\gamma_3\left(\frac{r_{\mathrm{M}}}{d_1}\right)^{\beta}\right)-\rho_{\mathrm{S}}'\gamma_3 y^{(2-\beta)}\mathcal{J}\left(\beta,-\Gamma_{\mathrm{M}}\gamma_3\left(\frac{r_{\mathrm{M}}}{y}\right)^{\beta}\right)+\rho_J\gamma_2 d_2^{(2-\beta)}\mathcal{J}\left(\beta,-\Gamma_{\mathrm{M}}\gamma_2\left(\frac{r_{\mathrm{M}}}{d_2}\right)^{\beta}\right)-$$

$$\left.\left.\rho_J\gamma_2 y^{(2-\beta)}\mathcal{J}\left(\beta,-\Gamma_{\mathrm{M}}\gamma_2\left(\frac{r_{\mathrm{M}}}{y}\right)^{\beta}\right)\right]-\rho_{\mathrm{M}}\pi r_{\mathrm{M}}^2\right) r_{\mathrm{M}} dr_{\mathrm{M}}. \tag{4.2.9}$$

Here, $\mathcal{L}_{I^{\mathrm{DL}}_{\phi_{\mathrm{S}},A^o_{\mathrm{M}}}} = \mathcal{L}_{I^{\mathrm{DL}}_{\phi_{\mathrm{S}},A^c_{\mathrm{M}}}}$ because ρ_{S} in A^c_{M} is approximately equal to ρ_{S} in A^o_{M}. γ_3 is the ratio of $P^{\mathrm{DL}}_{t,\mathrm{S}}$ and $P^{\mathrm{UL}}_{t,\nu}$ where $P^{\mathrm{DL}}_{t,\mathrm{S}}$ is the SBSs DL transmit power.

From (4.2.5), LT of MBS DL interference in A^o_{M}, i.e., $\mathcal{L}_{I^{\mathrm{UL}}_{\phi_{\mathrm{M}},A^o_{\mathrm{M}}}}$, is obtained as

$$\mathcal{L}_{I^{\mathrm{UL}}_{\phi_{\mathrm{M}},A^o_{\mathrm{M}}}}(s) =$$

$$= \exp\left(\frac{\rho_{\mathrm{M}}\pi\Gamma_{\mathrm{M}} d_2^{(2-\beta)} r_{\mathrm{M}}^{\beta}}{\beta/2-1}{}_2F_1\left(1,1-\frac{2}{\beta},2-\frac{2}{\beta},-\Gamma_{\mathrm{M}}\left(\frac{r_{\mathrm{M}}}{d_2}\right)^{\beta}\right)-\right.$$

$$\left.\frac{\rho_{\mathrm{M}}\pi\Gamma_{\mathrm{M}} d_1^{(2-\beta)} r_{\mathrm{M}}^{\beta}}{\beta/2-1}{}_2F_1\left(1,1-\frac{2}{\beta},2-\frac{2}{\beta},-\Gamma_{\mathrm{M}}\left(\frac{r_{\mathrm{M}}}{d_1}\right)^{\beta}\right)\right). \tag{4.2.7}$$

UL coverage probability expression, $P^{\mathrm{UL},*}_{A^c_{\mathrm{M}}}(\Gamma_{\mathrm{M}})$, having uniformly distributed IJs with RFA for MBS associated ν in A^c_{M} may be given as

$$P^{\mathrm{UL},*}_{A^c_{\mathrm{M}}}(\Gamma_{\mathrm{M}}) = \int_y^{d_1} \mathcal{L}_{I^{\mathrm{UL}}_{\phi_{\mathrm{M}},A^c_{\mathrm{M}}}}(s) \times \mathcal{L}_{I^{\mathrm{DL}}_{\phi_{\mathrm{S}},A^o_{\mathrm{M}}}}(s) \times \mathcal{L}_{I_{J,A}}(s)\, f_{r_{\mathrm{M},\nu}|\nu_{A^c_{\mathrm{M}}}}(r_{\mathrm{M},\nu})\, dr_{\mathrm{M},\nu}. \quad (4.2.10)$$

By putting (4.1.6), (4.1.7), (4.2.5) and (4.2.6), in (4.2.10), $P^{\mathrm{UL},*}_{A^c_{\mathrm{M}}}(\Gamma_{\mathrm{M}})$ is expressed as (4.2.8).

UL coverage probability expression, $P^{\mathrm{UL},*}_{A^o_{\mathrm{M}}}(\Gamma_{\mathrm{M}})$, having uniformly distributed IJs with RFA for MBS associated ν in A^o_{M}, may be given as

$$P^{\mathrm{UL},*}_{A^o_{\mathrm{M}}}(\Gamma_{\mathrm{M}}) = \int_{d_1}^{d_2} \mathcal{L}_{I^{\mathrm{UL}}_{\phi_{\mathrm{M}},A^o_{\mathrm{M}}}}(s) \times \mathcal{L}_{I^{\mathrm{DL}}_{\phi_{\mathrm{S}},A^c_{\mathrm{M}}}}(s) \times \mathcal{L}_{I_{J,A}}(s)\, f_{r_{\mathrm{M},\nu}|\nu_{A^o_{\mathrm{M}}}}(r_{\mathrm{M},\nu})\, dr_{\mathrm{M},\nu}. \quad (4.2.11)$$

By putting (4.1.6), (4.1.8), (4.2.6) and (4.2.7) in (4.2.11), $P^{\mathrm{UL},*}_{A^o_{\mathrm{M}}}(\Gamma_{\mathrm{M}})$ is expressed as (4.2.9).

Chapter 5

Results and Discussions

This chapter explains results of probabilities of UL coverage for ν in following conditions
(i) Probability without RFA.
(ii) Probability with RFA.
MATLAB 2017a was used to obtain the results. MBS, SBS, user and IJ are treated as

$A = (500\text{ m})^2\pi$,s.t.
$A = A^c_{\mathrm{M}} \mathrm{U} A^o_{\mathrm{M}}$

Distribution of IJs is in following area
$A = \pi(50\text{ m})^2$,s.t.

In addition, the transmitting powers of MBS=60 dBm, SBS=40 dBm, ν=20 dBm and IJs=20 dBm. Different variables, such as $P^{\mathrm{UL}}_{t,\nu}$, ρ_J, ρ_{M}, ρ_{S}, Γ_{M}, and $P_{t,J}$, are analyzed for location of ν in A^o_{M} against UL coverage.

5.1 Comparison of Probability of UL Coverage in A^o_{M} vs Γ_{M}

Fig. 5.1 compares the probabilities of UL coverage in A^o_{M} againts Γ_{M}. It can be seen that increase in the value of ρ_J leads to increase in IJs-I and decrease in coverage. Decrease in value of ρ_J improves the coverage. Therefore, the value of ρ_J is inversely proportional

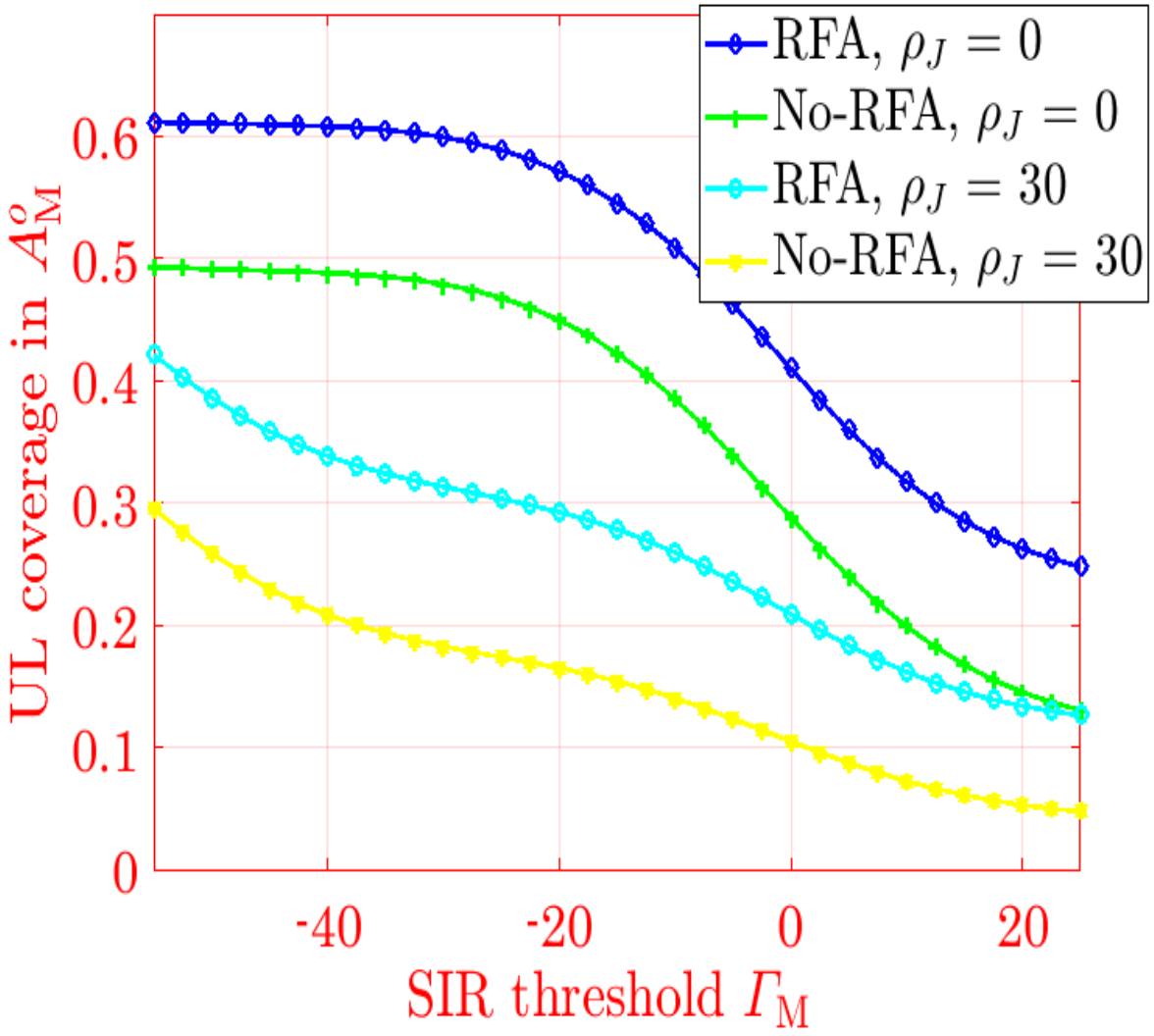

Figure 5.1: UL coverage versus Γ_M in A^o_M.

to coverage. In addition, Fig. 5.1 shows that employment with RFA improves coverage in presence as well as absence of IJs because the separation between the users utilizing same sub-band increases.

It can be seen in the Fig. 5.1 that with no RFA when ρ_J=0 , the value of UL coverage starts from 0.5 and reduces to around 0.2 whereas when ρ_J=30 the value starts from 0.3 and reduces to around 0.05. This shows that the with high value of ρ_J the coverage reduces. Moreover, with RFA when ρ_J=0 , the value of UL coverage starts from 0.6 and reduces to around 0.3 whereas when ρ_J=30 the value starts from 0.4 and reduces to around 0.2. Therefore, use of RFA has significant impact on UL coverage.

5.2 Comparison of Probability of UL Coverage in A_{M}^{o} vs Γ_{M} and ρ_J threshold

Fig. 5.2 measures the probabilities of UL coverage in A_{M}^{o} versus different values of the Γ_{M} and ρ_J threshold generated for ρ_J = 0, 20, 40, 60, 80, 100. It can be seen that RFA improves the coverage because of RFA's efficient use of the resources and effective mitigation of interference. Increasing ρ_J also causes severe degradation of UL coverage due to significant IJs-I.

It can be seen in the Fig. 5.2 that when ρ_J=0 , the value of UL coverage starts from 0.6 and reduces to around 0.3. When the value of ρ_J=20, the value of UL coverage starts from 0.5 and reduces to around 0.2. When the value of ρ_J=40, the value of UL coverage starts from 0.4 and reduces to around 1.5. When the value of ρ_J=60, the value of UL coverage starts from 0.3 and reduces to around 0.1. When the value of ρ_J=80, the value of UL coverage starts from 0.25 and reduces to around 0.05. When the value of ρ_J=100, the value of UL coverage starts from 0.2 and reduces to around 0.03. It can be deduced from the figure that the quality of coverage reduces with increasing value of ρ_J.

5.3 Comparison of UL coverage probabilities in A_{M} vs different IJs area radius

At Figs. 5.3 and 5.4, while assuming Γ_{M} = -40 dB and ρ_J = 20, 40, 60, 80 and 100, UL coverage probability in A_{M} is compared against IJs distribution area radius values. Plots have been generated by considering multiple plausible scenarios with and without RFA. It can be concluded from the results that increasing the distribution area of the IJs results in improvement in UL coverage because of reduction in number of IJs per unit area, making IJs less efficient as long as their transmission power is constant. Furthermore, due to efficient resource allocation RFA employment improves UL coverage.

Fig. 5.3 shows comparison between UL coverage and IJs distribution area for different values of ρ_J considering RFA. When the value of ρ_J=20, the value of UL coverage increases from 0 to 0.6 with increase in IJs distribution area upto 6. When the value of

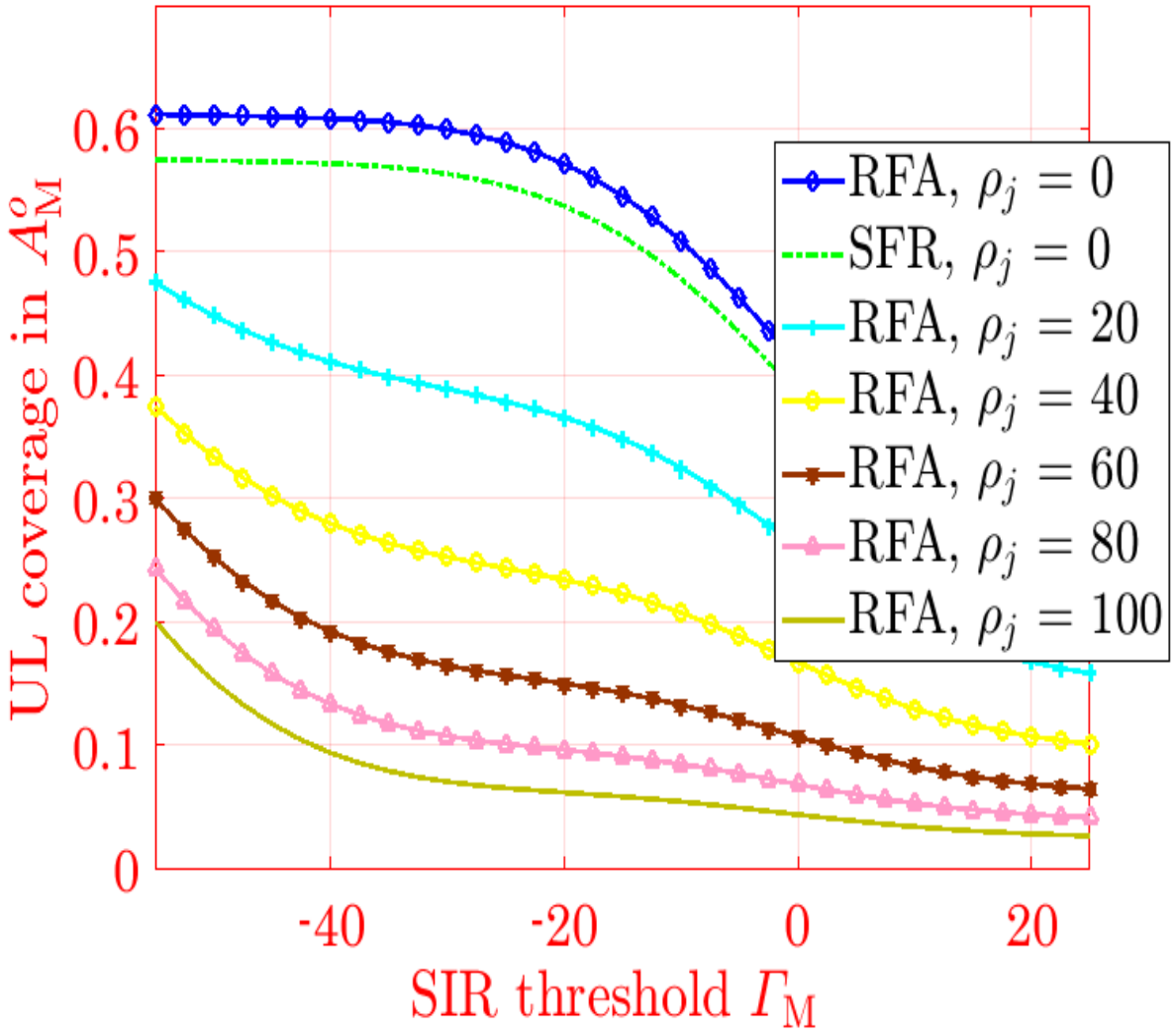

Figure 5.2: UL coverage against Γ_M and ρ_J in A^o_M.

ρ_J=40, the value of UL coverage increases from 0 to 0.59. When the value of ρ_J=60, the value of UL coverage increases from 0 to 0.58. When the value of ρ_J=80, the value of UL coverage increases from 0 to 0.57. When the value of ρ_J=100, the value of UL coverage increases from 0 to 0.56. It can be concluded that UL coverage improves as the IJs distribution area is increased.

Fig. 5.4 shows comparison between UL coverage and IJs distribution area for different values of ρ_J without RFA. When the value of ρ_J=20, the value of UL coverage increases from 0 to 0.48 with increase in IJs distribution area upto 6. When the value of ρ_J=40,

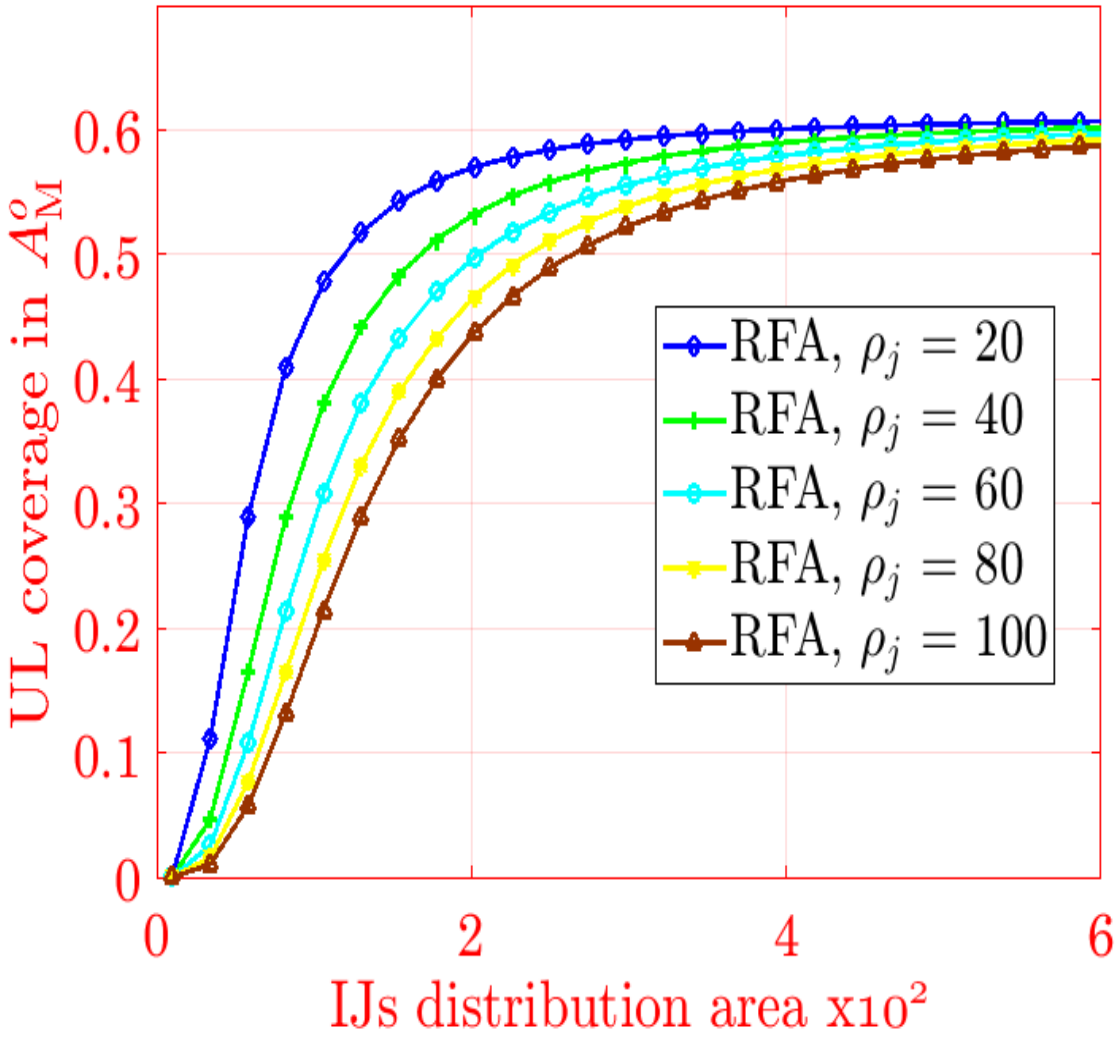

Figure 5.3: UL coverage against radius for IJs distribution area, with RFA.

the value of UL coverage increases from 0 to 0.47. When the value of ρ_J=60, the value of UL coverage increases from 0 to 0.46. When the value of ρ_J=80, the value of UL coverage increases from 0 to 0.45. When the value of ρ_J=100, the value of UL coverage increases from 0 to 0.44. Therefore, it can be inferred that increase in distribution area of IJs results in better UL coverage.

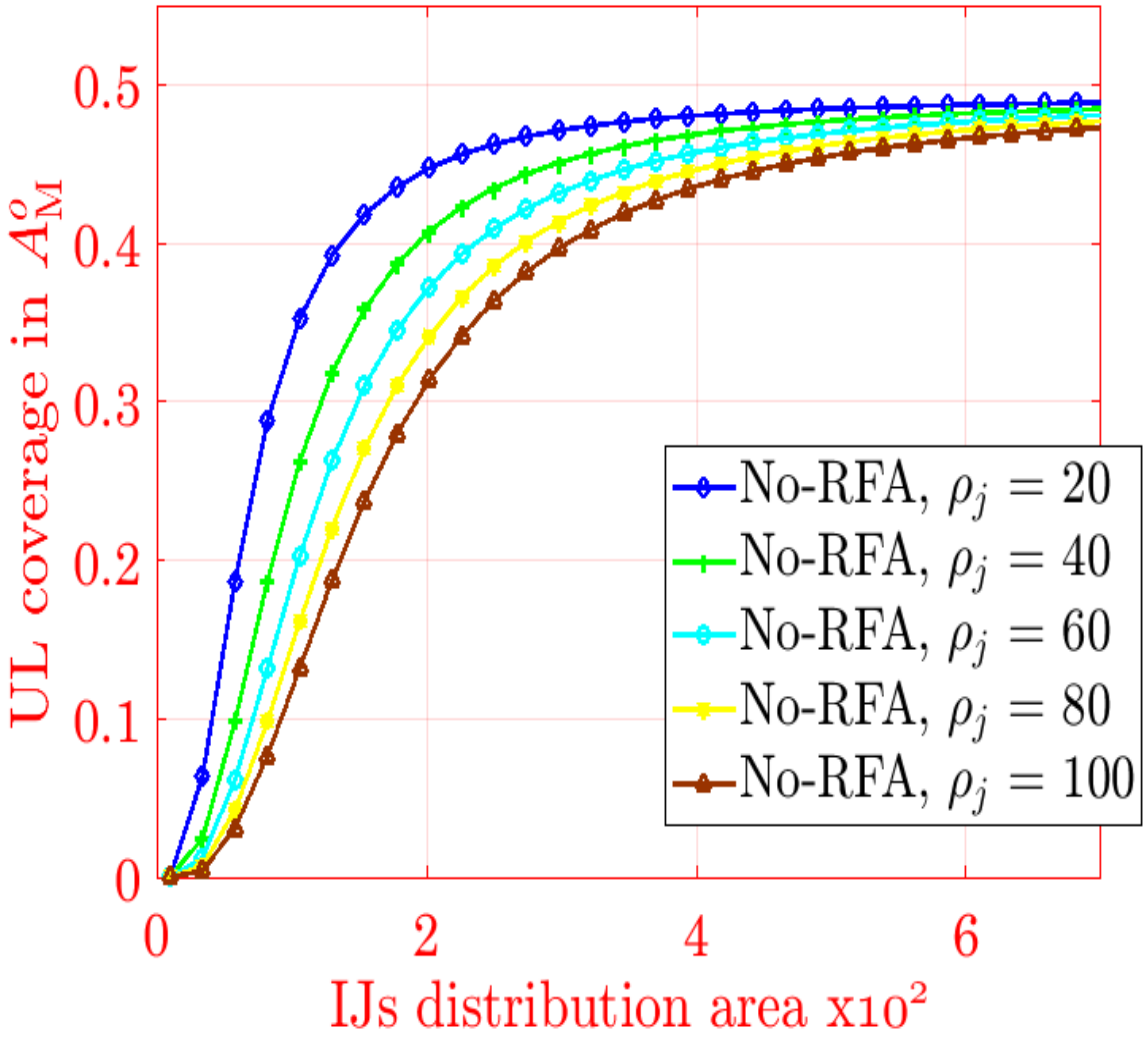

Figure 5.4: UL coverage against radius for IJs distribution area, without employing RFA.

5.4 Comparison of UL coverage probabilities in A_{M}^{o} vs different IJs area radius

The Figs. 5.5 and 5.6 calculate UL coverage probabilities in A_{M}^{o} versus different IJs distribution area radius values while assuming $\rho_J = 60$ and Γ_{M} = -60, -40, -20, 0 and 20. Multiple scenarios with and without RFA have been considered while generating the plots. The increase in the area of IJs distribution reduces IJs-I because of wider distances. Results show that, due to lower IJs-I, an increase in the distribution area of the IJs results in improved UL coverage. Furthermore, increase in the values of Γ_{M} reduces UL coverage because of lower user association.

Fig. 5.5 shows comparison between UL coverage and IJs distribution area for different values of Γ_M considering RFA. When the value of Γ_M=-60, the value of UL coverage increases from 0 to 0.6 with increase in IJs distribution area upto 8. When the value of Γ_M=-40, the value of UL coverage increases from 0 to 0.59. When the value of Γ_M=-20, the value of UL coverage increases from 0 to 0.55. When the value of Γ_M=0, the value of UL coverage increases from 0 to 0.35. When the value of Γ_M=20, the value of UL coverage increases from 0 to 0.2. It can be deduced that UL coverage is directly propositional to IJs distribution area.

Fig. 5.6 shows comparison between UL coverage and IJs distribution area for different values of Γ_M without RFA. When the value of Γ_M=-60, the value of UL coverage increases from 0 to 0.5 with increase in IJs distribution area upto 8. When the value of Γ_M=-40, the value of UL coverage increases from 0 to 0.48. When the value of Γ_M =-20, the value of UL coverage increases from 0 to 0.43. When the value of Γ_M=0, the value of UL coverage increases from 0 to 0.23. When the value of Γ_M =20, the value of UL coverage increases from 0 to 0.1. Therefore, results indicate that better UL coverage is achieved with increase in distribution area of IJs.

5.5 Discussion

Analysis of detailed results show that performance of the system has improved considerably with addition of RFA. UL coverage is improved significantly by using RFA in the presence of IJs. Therefore, the proposed method of using RFA has considerably reduced the effect of IJs on the UL communication.

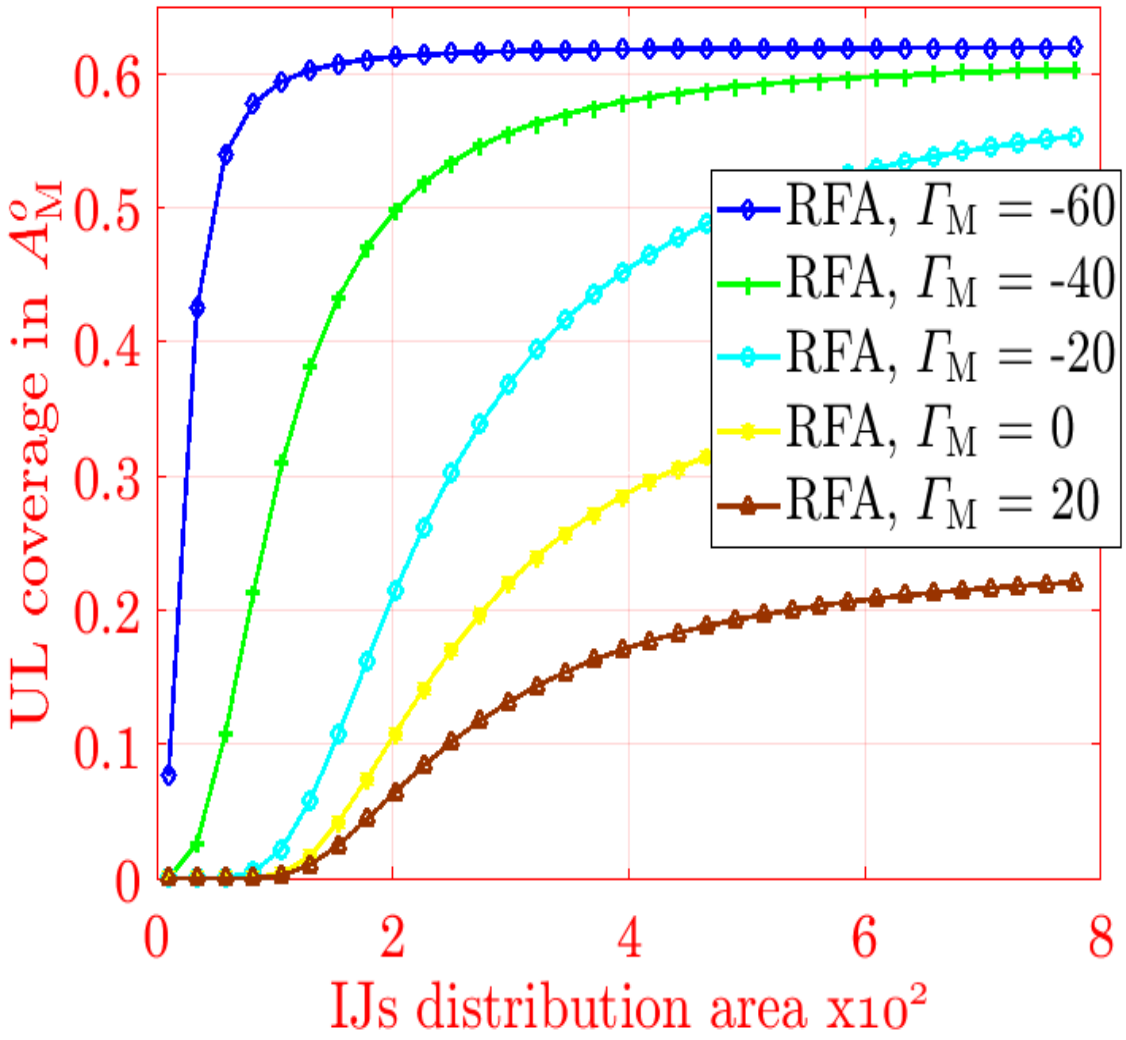

Figure 5.5: UL coverage against radius for IJs distribution area, with RFA.

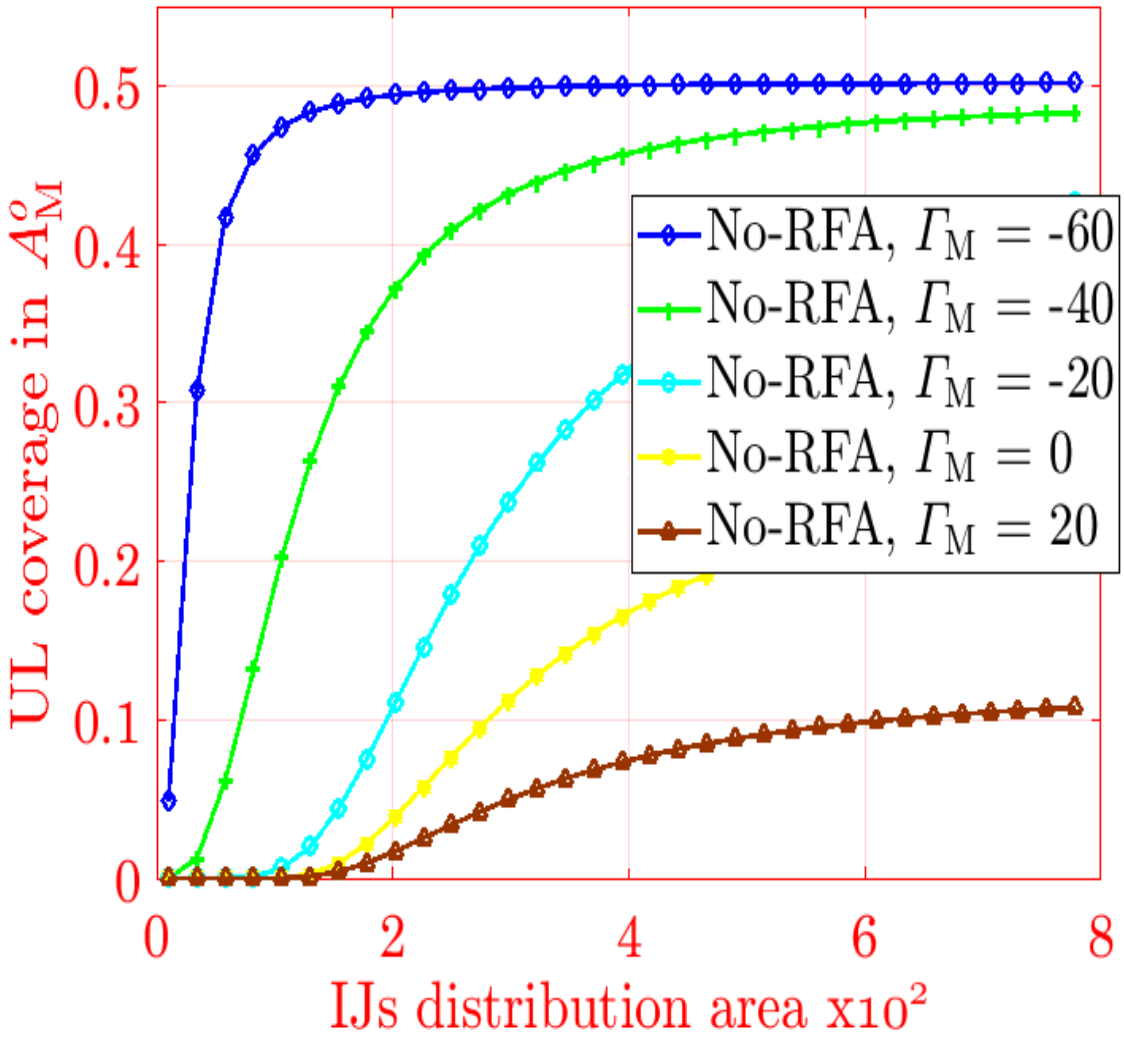

Figure 5.6: UL coverage against radius for IJs distribution area, without employing RFA.

Conclusion

Traditional homogeneous networks are facing significant challenges due to increase in data traffic. Therefore, Hetnets are required to cater for the increase in data traffic demand. Hetnets will be faced with more DDoS attacks because of growing reliance on data. IJs are one of the more effective methods of targeting mobile users with DDoS attacks. IJs are focusing on a wide band which distributes the energy over complete band and reduces strength over the target frequency. Strength of DL signals make it difficult to be targeted by IJs. Hence, UL signals are more susceptible to be a target of IJs attack. ICI is also one of the limiting factors which seriously degrades the performance of a HetNet because of multi-tier deployment and aggressive reuse of frequency. A proactive interference management scheme of RFA has been used in this paper to reduce the effects of IJs and ICI.

UL coverage of multi-tier HetNets was discussed, in the case of ICI and IJs-I intervention. This thesis assumes standardized deployment of MBSs, SBSs, users, and IJs employing IHPPPs. Evaluation of various parameters of the network, such as IJs' transmit power, distance, distribution area and SIR threshold with and without RFA jobs were used to obtain the results. Findings demonstrate that UL distribution reduces with the rise in strength and intensity conveyed by IJs. Furthermore, the investigations also indicate a higher SIR level reducing the UL area. In addition, owing to improved ICI and IJs-I reduction, it was found that RFA results in improved UL coverage in comparison with No-RFA case. Future work can be expended to include decoupled user associations to further reduce ICI and IJs-I and, thus, improve UL coverage.

Appendix A

A.1 Proof of LT of (4.1.4)

Proof of (4.1.4):

LT of the interference received from MBS-tier, $\mathcal{L}_{I_{\mathrm{M},A}}(s)$, in A, can be written as

$$\mathcal{L}_{I_{\mathrm{M},A}}(s) = \mathrm{E}_{I_{\mathrm{M},A}}\left[\exp\left(-I_{\mathrm{M},A}s\right)\right]\Big|_{s=\frac{r_{\mathrm{M}}^{\beta}\Gamma_{\mathrm{M}}}{P_{t,\nu}^{\mathrm{UL}}}}$$

$$= \mathrm{E}_{I_{\mathrm{M},A},|h_l|^2}\left[\exp\left(-s\sum_{l\in\phi_{\mathrm{M}}}P_{t,\mathrm{M}}|h_l|^2 r_l^{-\beta}\right)\right]$$

$$\overset{(a)}{\approx} \mathrm{E}_{I_{\mathrm{M},A},|h_l|^2}\left[\prod_{l\in\phi_{\mathrm{M}}}\exp\left(-|h_l|^2\gamma_{\circ}\Gamma_{\mathrm{M}}r_{\mathrm{M}}^{\beta}r_l^{-\beta}\right)\right]$$

$$\overset{(b)}{\approx} \mathrm{E}_{I_{\mathrm{M},A}}\left[\prod_{l\in\phi_{\mathrm{M}}}\mathrm{E}_{|h_l|^2}\exp\left(-|h_l|^2\gamma_{\circ}\Gamma_{\mathrm{M}}r_{\mathrm{M}}^{\beta}r_l^{-\beta}\right)\right]$$

$$\overset{(c)}{\approx} \mathrm{E}_{I_{\mathrm{M},A}}\left[\prod_{l\in\phi_{\mathrm{M}}}\frac{1}{1+\gamma_{\circ}\Gamma_{\mathrm{M}}\left(\frac{r_l}{r_{\mathrm{M}}}\right)^{-\beta}}\right]$$

$$\overset{(d)}{\approx} \exp\left(-2\pi\rho_{\mathrm{M}}\int_y^{d2}\frac{r_l dr_l}{1+\left(\frac{r_l}{\left(\gamma_{\circ}\Gamma_{\mathrm{M}}\right)^{1/\beta}r_{\mathrm{M}}}\right)^{\beta}}\right)$$

$$\overset{(e)}{\approx} \exp\left(-\pi\rho_{\mathrm{M}}\left(\gamma_{\circ}\Gamma_{\mathrm{M}}\right)^{2/\beta}r_{\mathrm{M}}^2\int_{\left(\frac{y}{\left(\gamma_{\circ}\Gamma_{\mathrm{M}}\right)^{1/\beta}r_{\mathrm{M}}}\right)^2}^{\left(\frac{d_2}{\gamma_{\circ}\Gamma_{\mathrm{M}}^{1/\beta}r_{\mathrm{M}}}\right)^2}\frac{du}{1+(u)^{\beta/2}}\right)$$

Here, Step (a) can be approached by putting value of s, Step (c) can be approached by calculating LT of Step (b) w.r.t h_j, Step (d) can be approached by utilizing proba-

bility generating functional (PGFL) of IHPPP [43], Step (e) is approached by putting $u = \left(\frac{r_l}{(\gamma_\circ \Gamma_{\mathrm{M}})^{1/\beta} r_{\mathrm{M}}} \right)^2$ in Step (d). Finally, (4.1.4) is approached by calculating Gauss-hypergeometric approximation of Step (e).

A.2 Proof of the LT of (4.2.5)

Proof of (4.2.5):

$$\begin{aligned}
\mathcal{L}_{I^{\mathrm{UL}}_{\phi_{\mathrm{M}}, A^c_{\mathrm{M}}}}(s) &= \mathrm{E}_{I^{\mathrm{UL}}_{\phi_{\mathrm{M}}, A^c_{\mathrm{M}}}} \left[\exp\left(-I^{\mathrm{UL}}_{\phi_{\mathrm{M}}, A^c_{\mathrm{M}}} s \right) \right] \Big|_{s = \frac{r_{\mathrm{M}}^{\beta} \Gamma_{\mathrm{M}}}{P^{\mathrm{UL}}_{t,\nu}}} \\
&= \mathrm{E}_{I^{\mathrm{UL}}_{\phi_{\mathrm{M}}, A^c_{\mathrm{M}}}, |h_l|^2} \left[\exp\left(-s \sum_{l \in \phi_{\mathrm{M}}} P^{\mathrm{UL}}_{t,\nu} |h_l|^2 r_l^{-\beta} \right) \right] \\
&= \mathrm{E}_{I^{\mathrm{UL}}_{\phi_{\mathrm{M}}, A^c_{\mathrm{M}}}, |h_l|^2} \left[\prod_{l \in \phi_{\mathrm{M}}} \exp\left(-|h_l|^2 \Gamma_{\mathrm{M}} r_{\mathrm{M}}^{\beta} r_l^{-\beta} \right) \right] \\
&= \mathrm{E}_{I^{\mathrm{UL}}_{\phi_{\mathrm{M}}, A^c_{\mathrm{M}}}} \left[\prod_{l \in \phi_{\mathrm{M}}} \mathrm{E}_{|h_l|^2} \exp\left(-|h_l|^2 \Gamma_{\mathrm{M}} r_{\mathrm{M}}^{\beta} r_l^{-\beta} \right) \right] \\
&= \mathrm{E}_{I^{\mathrm{UL}}_{\phi_{\mathrm{M}}, A^c_{\mathrm{M}}}} \left[\prod_{l \in \phi_{\mathrm{M}}} \frac{1}{1 + \Gamma_{\mathrm{M}} \left(\frac{r_l}{r_{\mathrm{M}}} \right)^{-\beta}} \right] \\
&= \exp\left(-2\pi \rho_{\mathrm{M}} \int_y^{d_1} \frac{r_l dr_l}{1 + \left(\frac{r_l}{\Gamma_{\mathrm{M}}^{1/\beta} r_{\mathrm{M}}} \right)^{\beta}} \right) \\
&\overset{(f)}{\approx} \exp\left(-\pi \rho_{\mathrm{M}} \Gamma_{\mathrm{M}}^{2/\beta} r_{\mathrm{M}}^2 \int_{\left(\frac{y}{\Gamma_{\mathrm{M}}^{1/\beta} r_{\mathrm{M}}} \right)^2}^{\left(\frac{d_1}{\Gamma_{\mathrm{M}}^{1/\beta} r_{\mathrm{M}}} \right)^2} \frac{du}{1 + (u)^{\beta/2}} \right)
\end{aligned}$$

Finally, we obtain (4.2.5) by calculating Gauss-hypergeometric approximation of Step (f).

References

[1] D. B. Da Costa, T. Q. Duong, M. A. Imran, H. Q. Ngo, N. Yang, and O. A. Dobre, "Modeling, analysis, and design of 5G ultra-dense networks," *IEEE Access*, vol. 7, pp. 18 894–18 898, 2019.

[2] J. G. Andrews, S. Buzzi, W. Choi, S. V. Hanly, A. Lozano, A. C. Soong, and J. C. Zhang, "What will 5G be?" *IEEE Journal on Selected Areas in Communications*, vol. 32, no. 6, pp. 1065–1082, 2014.

[3] B. Błaszczyszyn, M. Haenggi, P. Keeler, and S. Mukherjee, *Stochastic Geometry Analysis of Cellular Networks*. Cambridge University Press, 2018.

[4] M. S. Akhtar, Z. H. Abbas, F. Muhammad, and G. Abbas, "Analysis of decoupled association in HetNets using soft frequency reuse scheme," *AEU - International Journal of Electronics and Communications*, vol. 113, p. 152961, 2020.

[5] J. Mirkovic and P. Reiher, "A taxonomy of ddos attack and ddos defense mechanisms," *ACM SIGCOMM Computer Communication Review*, vol. 34, no. 2, pp. 39–53, 2004.

[6] R. P. Jover, "Security attacks against the availability of LTE mobility networks: Overview and research directions," in *proc. International Symposium on Wireless Personal Multimedia Communication (WPMC)*. IEEE, 2013, pp. 1–9.

[7] Y. Huo, X. Fan, L. Ma, X. Cheng, Z. Tian, and D. Chen, "Secure communications in tiered 5G wireless networks with cooperative jamming," *IEEE Trans. on Wireless Commun.*, 2019.

[8] W. Jundong, "Complex environment noise barrage jamming effects on airborne warning radar," *American J. of Remote Sensing*, vol. 6, no. 2, pp. 59–63, 2018.

[9] A. Viterbi, "A robust ratio-threshold technique to mitigate tone and partial band jamming in coded MFSK systems," in *proc. MILCOM 1982-IEEE Military Communications Conference-Progress in Spread Spectrum Communications*, vol. 1. IEEE, 1982, pp. 22–4.

[10] M. S. Haroon, S. Ahmad, and J. A. Khan, "LLR-based erasure decoding of SFH-MFSK in the presence of tone jamming," in *proc. 11th International Bhurban Conference on Applied Sciences & Technology (IBCAST)*. IEEE, 2014, pp. 453–457.

[11] F. Girke, F. Kurtz, N. Dorsch, and C. Wietfeld, "Towards resilient 5G: Lessons learned from experimental evaluations of LTE uplink jamming," in *2019 IEEE International Conference on Communications Workshops (ICC Workshops)*. IEEE, 2019, pp. 1–6.

[12] C. V. Ham and T. E. Scoughton, "Radio frequency jammer," Jan. 15 2008, uS Patent 7,318,368.

[13] S. Wang, Y. Gao, N. Sha, G. Zhang, and G. Zang, "Physical layer security in k-tier heterogeneous cellular networks over nakagami-m channel during uplink and downlink phases," *IEEE Access*, vol. 7, pp. 14 581–14 592, 2019.

[14] Z. H. Abbas, F. Muhammad, and L. Jiao, "Analysis of load balancing and interference management in heterogeneous cellular networks," *IEEE Access*, vol. 5, pp. 14 690–14 705, 2017.

[15] B. Soret, A. De Domenico, S. Bazzi, N. H. Mahmood, and K. I. Pedersen, "Interference coordination for 5G new radio," *IEEE Wireless Communications*, vol. 25, no. 3, pp. 131–137, 2017.

[16] S. Zou, N. Liu, Z. Pan, and X. You, "Joint power and resource allocation for non-uniform topologies in heterogeneous networks," in *proc. 83rd Vehicular Technology Conference (VTC Spring)*. IEEE, 2016, pp. 1–5.

[17] T. Han, J. Gong, X. Liu, S. R. Islam, Q. Li, Z. Bai, and K. S. Kwak, "On downlink NOMA in heterogeneous networks with non-uniform small cell deployment," *IEEE Access*, vol. 6, pp. 31 099–31 109, 2018.

[18] M. S. Haroon, Z. H. Abbas, G. Abbas, and F. Muhammad, "Analysis of interference mitigation in heterogeneous cellular networks using soft frequency reuse

and load balancing," in *proc. 28th International Telecommunication Networks and Applications Conference (ITNAC)*. IEEE, 2018, pp. 1–6.

[19] ——, "Coverage analysis of ultra-dense heterogeneous cellular networks with interference management," *Wireless Networks*, pp. 1–13, 2019.

[20] S. Hashima, O. Muta, M. Alghonimey, H. Shalaby, H. Frukawa, S. Elnoubi, and I. Mahmoud, "Area spectral efficiency performance comparison of downlink fractional frequency reuse schemes for MIMO heterogeneous networks," in *proc. International Conference on Information Science, Electronics and Electrical Engineering*, vol. 2. IEEE, 2014, pp. 1005–1010.

[21] M. Lichtman, J. D. Poston, S. Amuru, C. Shahriar, T. C. Clancy, R. M. Buehrer, and J. H. Reed, "A communications jamming taxonomy," *IEEE Security and Privacy*, vol. 14, no. 1, pp. 47–54, 2016.

[22] S. Gecgel, C. Goztepe, and G. K. Kurt, "Jammer detection based on artificial neural networks: A measurement study," in *Proc. of the ACM Workshop on Wireless Security and Machine Learning*, 2019, pp. 43–48.

[23] L. Zhang, F. Restuccia, T. Melodia, and S. M. Pudlewski, "Jam sessions: Analysis and experimental evaluation of advanced jamming attacks in MIMO networks," in *Proc. of the Twentieth ACM International Symposium on Mobile Ad Hoc Networking and Computing*, 2019, pp. 61–70.

[24] T. T. Do, E. Björnson, E. G. Larsson, and S. M. Razavizadeh, "Jamming-resistant receivers for the massive mimo uplink," *IEEE Transactions on Information Forensics and Security*, vol. 13, no. 1, pp. 210–223, 2017.

[25] K. Grover, A. Lim, and Q. Yang, "Jamming and anti-jamming techniques in wireless networks: A survey," *Int. J. of Ad Hoc and Ubiquitous Comput.*, vol. 17, no. 4, pp. 197–215, 2014.

[26] S.-M. Tseng, Y.-F. Chen, P.-H. Chiu, and H.-C. Chi, "Jamming resilient cross-layer resource allocation in uplink harq-based simo ofdma video transmission systems," *IEEE Access*, vol. 5, pp. 24 908–24 919, 2017.

[27] M. M. Pervez, Z. H. Abbas, F. Muhammad, and L. Jiao, "Location-based coverage and capacity analysis of a two tier HetNet," *IET Communications*, vol. 11, no. 7, pp. 1067–1073, 2016.

[28] A. Ijaz, S. A. Hassan, S. A. R. Zaidi, D. N. K. Jayakody, and S. M. H. Zaidi, "Coverage and rate analysis for downlink HetNets using modified reverse frequency allocation scheme," *IEEE Access*, vol. 5, pp. 2489–2502, 2017.

[29] N. Hassan and X. Fernando, "Massive mimo wireless networks: An overview," *Electronics*, vol. 6, no. 3, p. 63, 2017.

[30] R. W. Heath, M. Kountouris, and T. Bai, "Modeling heterogeneous network interference using poisson point processes," *IEEE Transactions on Signal Processing*, vol. 61, no. 16, pp. 4114–4126, 2013.

[31] H. S. Dhillon, M. Kountouris, and J. G. Andrews, "Downlink mimo hetnets: Modeling, ordering results and performance analysis," *IEEE Transactions on Wireless Communications*, vol. 12, no. 10, pp. 5208–5222, 2013.

[32] W. Xu and H. Zhang, "Uplink interference mitigation for heterogeneous networks with user-specific resource allocation and power control," *EURASIP Journal on Wireless Communications and Networking*, vol. 2014, no. 1, p. 55, 2014.

[33] M. Hefnawi, "Hybrid beamforming for millimeter-wave heterogeneous networks," *Electronics*, vol. 8, no. 2, p. 133, 2019.

[34] N. Naganuma, S. Nakazawa, S. Suyama, Y. Okumura, and H. Otsuka, "Performance evaluation of adaptive control cre in hetnet with eicic scheme," *IEICE Communications Express*, vol. 6, no. 4, pp. 166–171, 2017.

[35] N. Deng, W. Zhou, and M. Haenggi, "Outage and capacity of heterogeneous cellular networks with intra-tier dependence," in *2014 Sixth International Conference on Wireless Communications and Signal Processing (WCSP)*. IEEE, 2014, pp. 1–5.

[36] A. Haider and S.-H. Hwang, "Maximum transmit power for ue in an lte small cell uplink," *Electronics*, vol. 8, no. 7, p. 796, 2019.

[37] H. Munir, S. A. Hassan, H. Pervaiz, Q. Ni, and L. Musavian, "User association in 5g heterogeneous networks exploiting multi-slope path loss model," in *2017 2nd*

Workshop on recent trends in telecommunications research (RTTR). IEEE, 2017, pp. 1–5.

[38] X. Zhang and J. G. Andrews, "Downlink cellular network analysis with multi-slope path loss models," *IEEE Transactions on Communications*, vol. 63, no. 5, pp. 1881–1894, 2015.

[39] L. Guo, S. Cong, and Z. Sun, "Multichannel analysis of soft frequency reuse and user association in two-tier heterogeneous cellular networks," *EURASIP Journal on Wireless Communications and Networking*, vol. 2017, no. 1, pp. 1–20, 2017.

[40] M. Fereydooni, M. Sabaei, M. Dehghan, G. B. Eslamlou, and M. Rupp, "Analytical evaluation of heterogeneous cellular networks under flexible user association and frequency reuse," *Computer Communications*, vol. 116, pp. 147–158, 2018.

[41] K.-H. Liu and T.-Y. Yu, "Performance of off-grid small cells with non-uniform deployment in two-tier HetNet," *IEEE Transactions on Wireless Communications*, vol. 17, no. 9, pp. 6135–6148, 2018.

[42] F. Muhammad, Z. H. Abbas, and F. Y. Li, "Cell association with load balancing in nonuniform heterogeneous cellular networks: Coverage probability and rate analysis," *IEEE Transactions on Vehicular Technology*, vol. 66, no. 6, pp. 5241–5255, 2016.

[43] X. Jiang, B. Zheng, W.-P. Zhu, L. Wang, and Y. Zou, "Large system analysis of heterogeneous cellular networks with interference alignment," *IEEE Access*, vol. 6, pp. 8148–8160, 2018.

[44] M. Haenggi, *Stochastic Geometry for Wireless Networks*. Cambridge University Press, 2012.

[45] M. S. Haroon, Z. H. Abbas, F. Muhammad, and G. Abbas, "Coverage analysis of cell-edge users in heterogeneous wireless networks using Stienen's model and RFA scheme," *International Journal of Communication Systems*, p. e4147.